



INTERNATIONAL ATOMIC ENERGY AGENCY
UNITED NATIONS EDUCATIONAL, SCIENTIFIC AND CULTURAL ORGANIZATION



INTERNATIONAL CENTRE FOR THEORETICAL PHYSICS
34100 TRIESTE (ITALY) - P.O. B. 589 - MIRAMARE - STRADA COSTIERA 11 - TELEPHONES: 224281/2/3/4/5/6
CABLE: CENTRATOM - TELEX 460392-I

SMR/111 - 27

SECOND SUMMER COLLEGE IN BIOPHYSICS

30 July - 7 September 1984

Lecture 1: Electron paramagnetic resonance of copper-proteins: Monte Carlo simulation of spectra.

Lecture 2: Molecular structure and dynamics of human ceruloplasmin.

S. CANNISTRARO
Gruppo di Biofisica Molecolare
Dipartimento di Fisica
Università degli Studi
Piazza dell'Università
06100 Perugia
Italy

These are preliminary lecture notes, intended only for distribution to participants.
Missing or extra copies are available from Room 230.

①

"Electron Paramagnetic Resonance of Copper-Proteins: Monte Carlo Simulation of Spectra".

Metal ions play an important role in the structure, dynamics and function of several biomolecules (Mg in photosynthesis, Fe in oxygen transport, etc...)

Generally, they occupy the so-called "active site" within the biomolecules requiring their presence. Metal ions then modulate the structure and function of the biomolecule and very often are involved in electron transfer mechanisms underlying the biochemical function of the molecule.

In particular, this is the case of most of the copper-containing enzymes.

It is obvious then the importance of the knowledge of the microenvironment of these ions.

Several spectroscopic techniques are currently available to study the

②

structure of the active site of metallo-proteins

In the case of paramagnetic ions (Cu^{2+} , Fe^{3+} , Co^{2+} , Mn^{2+} ...) EPR spectroscopy is highly sensitive to the symmetry and strength of the crystal field set up by the amino acid ligands belonging to the protein. Then a lot of information can be gained on the structure of the metal binding site by the analysis of EPR spectra.

EPR spectra arise from microwave radiation induced transitions between Zeeman levels which are determined by the interaction of the ion magnetic moment with an external magnetic field (H).

In a general way, the EPR spectra of a copper (Cu^{2+}) complex can be interpreted in terms of the spin Hamiltonian:

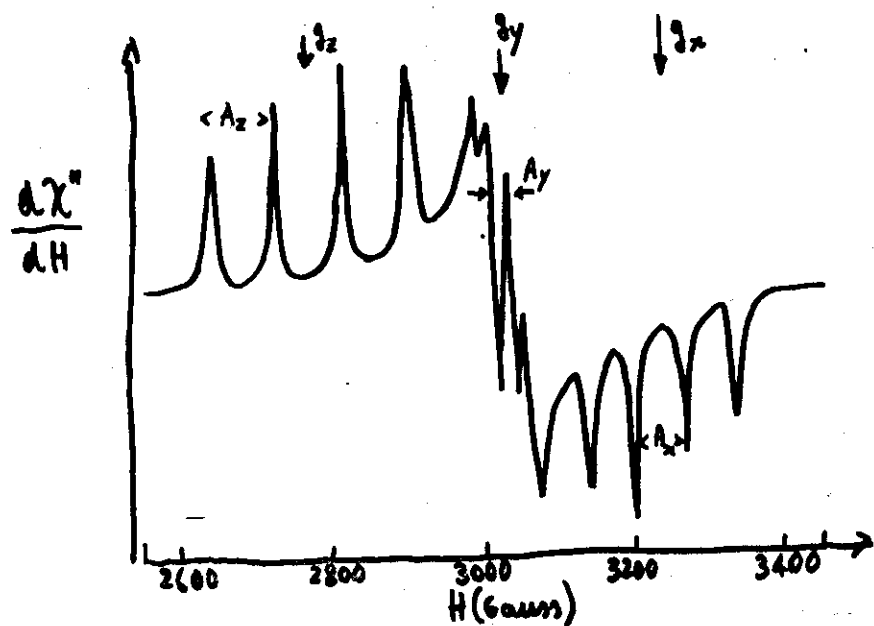
$$\mathcal{H} = \underbrace{\beta \vec{H} \cdot \vec{g} \cdot \vec{S}}_{\text{Zeeman}} + \underbrace{\vec{S} \cdot \vec{A} \cdot \vec{I}}_{\text{hyperfine}} \quad \text{with } S = \frac{1}{2}; I = \frac{3}{2}$$

or:

$$\textcircled{3} \quad \mathcal{H} = \beta \left[H_z g_z S_z + H_x g_x S_x + H_y g_y S_y \right] + S_z A_z I_z + S_x A_x I_x + S_y A_y I_y$$

where $g_{x,y,z}$, $A_{x,y,z}$ are the g -values and hyperfine components respect to the molecular axes (\hat{g} , \hat{A} tensors diagonal)

From a polycrystalline sample or from a frozen solution (biological) the following EPR pattern is obtained:

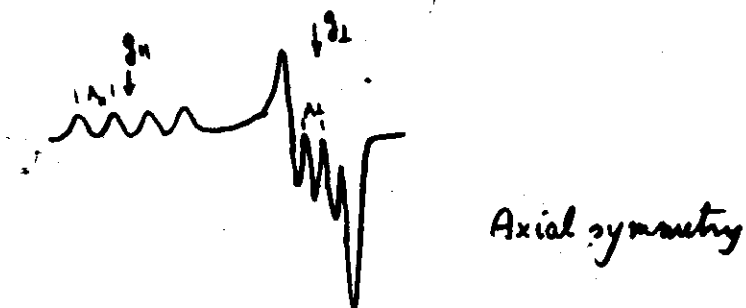


Very often an axial symmetry is displayed by the ligands around the Cu^{++} ion and in this case the spin Hamiltonian takes the form:

$$\textcircled{4} \quad \mathcal{H} = \beta \left[H_z g_z S_z + g_{\perp} (H_x S_x + H_y S_y) \right] + A_{\parallel} S_z I_z + A_{\perp} (S_x I_x + S_y I_y)$$

$$g_z = g_{\parallel}; \quad g_x = g_y = g_{\perp}; \quad A_z = A_{\parallel}; \quad A_x = A_y = A_{\perp}$$

A typical pattern arising from a copper complex in frozen solution is then:

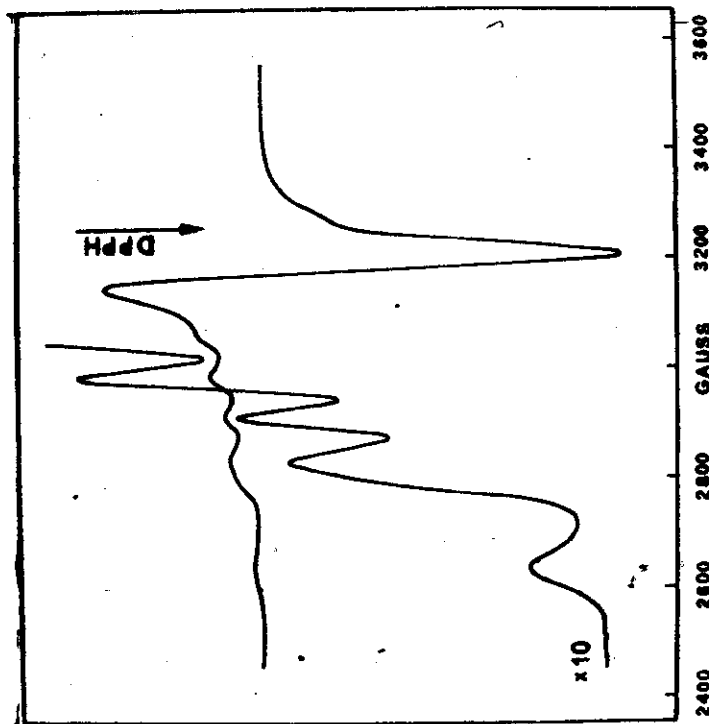


More often, copper proteins show low temperature EPR spectra with lower resolution in the g_{\perp} -region, and which results from the superposition of different patterns due to Cu^{++} ions in different microenvironments.

This was the case for Ceruloplasmin (CP)

- human plasma protein with oxidase activity
- M.W. $\approx 132,000$ daltons
- about 7 copper ions are bound to CP; 3 of them are paramagnetic, 4 are probably coupled antiferromagn.

EPR spectrum of $\text{Ce}^{+}\text{Eu}^{3+}$. $T = 77\text{K}$.



Why Simulation

To simulate the EPR patterns of CP we have solved the orthorhombic spin Hamiltonian obtaining the following magnetic field values for the allowed EPR transitions:

$$H = H_0 - \frac{KM_I}{g\beta} - \frac{1}{g^2\beta^2H_0} \left[\frac{A_x^2 A_y^2}{4B^2} + \frac{A_z^2 B^2}{4K^2} + A_z g_x^2 g_y^2 g_z^2 (A_y^2 - A_x^2) \alpha^2 \cdot (1 - \alpha^2) \eta^2 \right] \cdot [I(I+1) - M_I^2] - \frac{1}{g^2\beta^2H_0} \left\{ \frac{1 - \eta^2}{2K^2 g^2} \left[\frac{g_z^2 g_x^2}{g^2} (A_z^2 - B^2) \right]^2 + \frac{g_x^2 g_y^2}{g^4} (A_x^2 - A_y^2)^2 \alpha^2 (1 - \alpha^2) \right\} M_I^2$$

Where:

$$H_0 = \frac{h\nu}{g\beta}; \quad g^2 = g'^2 + (g_z^2 - g'^2) \eta^2$$

$$g'^2 = g_y^2 + (g_x^2 - g_y^2) \alpha^2; \quad K^2 g^2 = A_z g_z^2 \eta^2 + B^2 g'^2 (1 - \eta^2)$$

$$g'^2 B^2 = g_y^2 A_y^2 + (g_x^2 A_x^2 - g_y^2 A_y^2) \alpha^2; \quad \alpha = \cos \varphi; \quad \eta = \cos \theta$$

For random orientation of the Eu^{2+} ion-bearing molecules (powders or frozen glasses) the absorption $A(H)$ of each hyperfine line is given by:

$$A(H) = (2I+1)^{-1} g^2 \sin \theta \left| \frac{d\theta d\varphi}{dH} \right|$$

where: $g_1^2 = \frac{1}{2} \left[\left(\frac{g_x g_z}{g} \right)^2 + g_y^2 \right]$ takes into account

(7) the variation of the transition probability with the direction of the applied field.

By summing over the values of φ and θ and assuming that the resonance has the shape $S(H)$ (whose derivative is $S'(H)$: experimental EPR spectra are usually displayed as the derivative of absorption) the derivative of the absorption at a field H_a is:

$$I(H_a) = \int S'(H_a - H) A(H) dH = (2I+1)^{-1} \int_0^{\pi/2} \int_0^{\pi} S'(H_a - H) \sin\theta d\theta d\varphi$$

the total derivative of the EPR absorption is obtained over all the hyperfine lines $(4: -\frac{3}{2}, 1: -\frac{1}{2}, 1: \frac{1}{2}, 4: \frac{3}{2})$

We have used Gaussian line-shapes:

$$S'(H) = 2\pi^{-1/2} \gamma^{-3} H e^{-(H/\gamma)^2}; \quad \gamma = 2^{-1/2} \Delta H$$

(ΔH being separation between maximum and minimum slope)

The expression used were programmed in Fortran 77 for a Prime computer.

The computer-synthesized EPR spectra were used to fit the experimental spectrum obtained at 77K from CP

According to the method of least-squares, the best fit was obtained by minimizing the function:

$$F(p) = \sum_{i=1}^N [I^{\text{exp}}(H_i) - I^{\text{th}}(H_i, p)]^2$$

(8) I^{exp} : derivative of total absorption sampled at $N=250$ points of the field.

I^{th} : model function which is non linear (transcendental) in its parameter p

The parameters taken into account were the g-values (g_x, g_y, g_z), the hyperfine couplings (A_x, A_y, A_z) and the line widths ($\Delta H_x, \Delta H_y, \Delta H_z$) of each type of Cu^{2+} paramagnetic center.

To fit the composite ^{experimental} spectrum of CP the theoretical line shape was considered as a sum:

$$I^{\text{th}}(H, p) = \sum_{i=1}^n \alpha_i I_i^{\text{th}}(H, p_i)$$

Where α_i are the molar fractions, the I_i^{th} are the normalized theoretical spectra of the n (3 in our case) different Cu^{2+} paramagnetic sites present in CP molecule and p_i are the subsets of parameters ($g, A, \Delta H$) each related to these theoretical spectra.

In order to be efficient, the least-squares method requires that the starting parameters p^0 approach the values p^* of the minimum $F(p)$ and in this case the values of the α_i

can be determined.

(9)

The experimental EPR spectra are too complicated to make a reliable estimate of all the spin hamiltonian parameters. Very often the only reasonable assumption which can be made is one about their possible range of variation.

In this respect the Monte Carlo method allows us to deal with the problem of minimizing the function $F(p)$ in a realistic way, so that meaningful evaluation of the p parameters can be obtained.

To run Monte Carlo simulation, we allowed each EPR parameter to vary over a wide range, consistent both with that estimated (where possible) from experimental spectra and with that reported in literature for each Cu^{2+} type.

Best fit of I^{exp} was obtained after running more than 100,000 histories.

Results : 10 , 11

Standard deviations of the parameters were calculated by the χ^2 method :

$$\chi^2 = \sum_{i=1}^N \left[\frac{I^{\text{exp}}(H_i) - I^{\text{th}}(H_i; p^*)}{\sigma_i} \right]^2$$

σ_i were calculated after repeated runs of the same exp. spectrum

(10)

Cp-Cu^{2+}

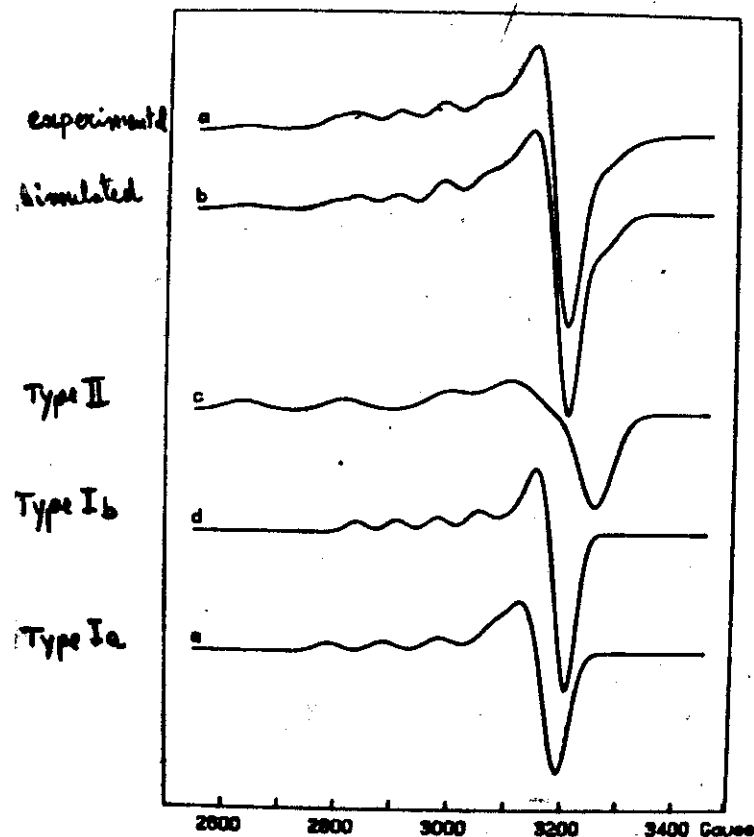
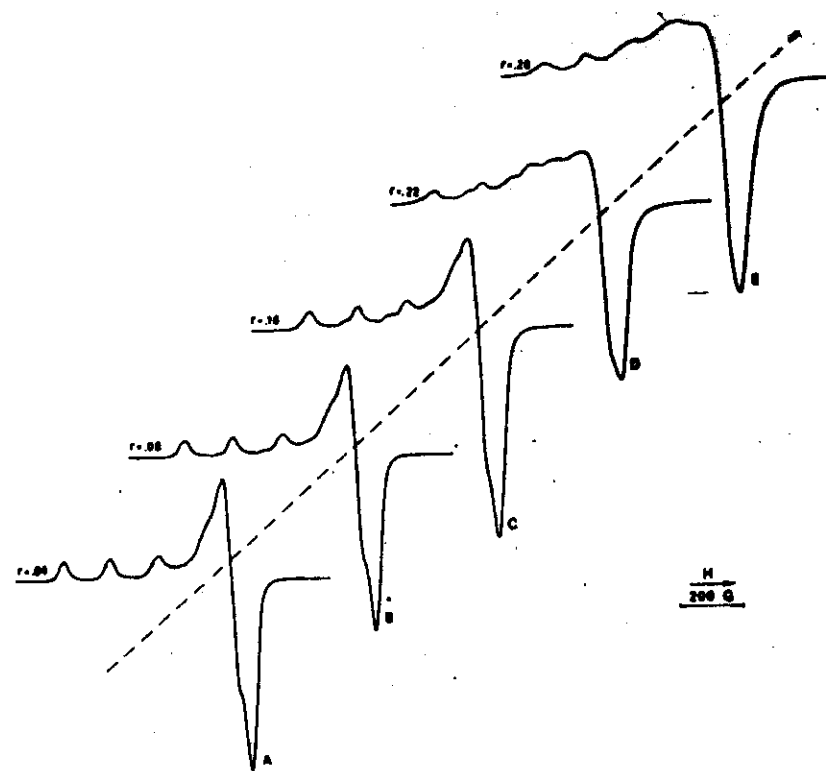


Table I. EPR parameters and molar fractions (2 standard deviation) related to the three spectroscopically different CP Cu²⁺ ions, as calculated by the best fit of the experimental data.

Parameter	Type II	Type Ia	Type Ib
$a_{\parallel} \text{ mG}$	2.2468 ± 0.0014	2.2227 ± 0.0013	2.2159 ± 0.0011
$a_{\perp} \text{ mG}$	2.0594 ± 0.0007	2.0432 ± 0.0005	2.0489 ± 0.0002
$A_{\parallel} \text{ mG}$	177.8 ± 1.5	96.1 ± 1.3	70.1 ± 0.7
$A_{\perp} \text{ mG}$	23.4 ± 1.5	9.6 ± 0.0	10.8 ± 0.5
$\Delta H_{\parallel} = 2A_{\parallel} - 2A_{\perp} \text{ mG}$	65.7 ± 2.0	43.8 ± 1.2	35.3 ± 0.6
Molar fraction	$d_1 = 0.39 \pm 0.01$	$d_2 = 0.27 \pm 0.05$	$d_3 = 0.29 \pm 0.01$



Spettri EPR del complesso Cu⁺⁺-tRNA registrati a vari valori di r.

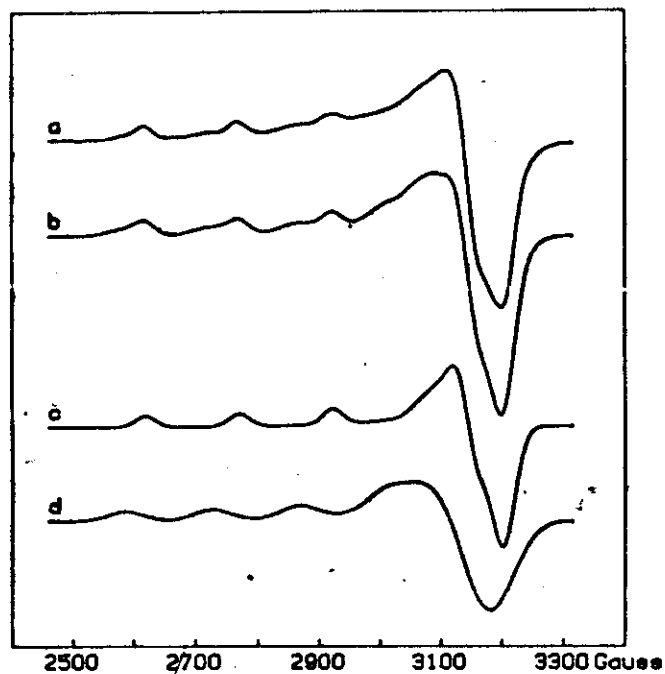
(13)

(14)

MONTE CARLO SIMULATION OF THE ELECTRON PARAMAGNETIC RESONANCE
SPECTRUM DISPLAYED BY COPPER CERULOPLASMIN AT 77 K

G. GIUGLIARELLI and S. CANNISTRARO

Gruppo di Biofisica Molecolare, Dipartimento di Fisica
dell' Università, Perugia, Italy



Abstract:

Human ceruloplasmin contains several intrinsic copper ions, some of them being paramagnetic. The presence of two classes of paramagnetic Cu^{2+} ions (Type I and Type II) has been suggested; the two types having significantly different spectroscopic features. However, there are conflicting reports both on the ratio of the number of Type I to Type II Cu^{2+} and on their EPR spectroscopic parameters.

By using a Monte Carlo method we obtained the best fit of the experimental spectrum with a synthesized composite spectrum generated by two Type I Cu^{2+} (Type Ia and Type Ib, possessing slightly different spin Hamiltonian parameters) and by one Type II Cu^{2+} . Correspondingly, the EPR spectroscopic parameters (*viz.* the g -tensors, hyperfine couplings, line-widths and molar fractions) together with their accuracies, were determined.

PACS NUMBERS: 76.30 -v; 87.15. -v

Introduction

Ceruloplasmin (CP) is a copper-containing protein showing many interesting features when studied from different points of view. It has been ascertained (1) that it is involved in several pathological stresses even though its enzymatic role is much debated (2,3). Moreover a very interesting electron tunneling process has been postulated to occur during the very complicated and almost unknown pathway leading to its oxidase activity (3,4). In addition a high-temperature "excitonic" superconductive catastrophe seems to occur when the protein is stored in the frozen state (5,6). Finally, well-defined intermolecular correlations, occurring at a range of about 110 \AA , have been observed when aqueous solutions of CP molecules are studied by small angle neutron scattering (7).

Indeed the spectroscopic features of CP are quite unusual among the biomolecules. From the optical point of view the protein is characterized by a very intense blue colour and the overall absorption spectrum seems to be a composite of several bands arising from distinct absorbing units, involving the immediate environment of the Cu^{2+} ions chelated to the protein.

As regards these ions, the extensive literature existing in the field reports a great variation in the number of Cu^{2+} ions present per molecule of CP. The main source of scattering around this value is attributable to the uncertainty about the molecular weight of the protein. However, a

reasonable consensus between the most recent data would suggest a molecular weight of about 134,000 with seven copper atoms per protein molecule (3,8). Some of these ions are in a paramagnetic state, while the rest are diamagnetic, probably consisting of Cu^{2+} ion pairs with extensive antiferromagnetic coupling (3).

Essentially, two classes of paramagnetic copper ions are observed in copper metallo-proteins (4). Type I Cu^{2+} ions are characterized by a strong optical absorption near 610 nm ($\epsilon_{610} \approx 10^4 \text{ M}^{-1} \text{ cm}^{-1}$), which endows the protein with blue colour, and an anomalously small hyperfine splitting constant ($A_h = 70 \pm 100 \text{ Gauss}$). The second class, designated as Type II Cu^{2+} , has the usual physical characteristic of a simple cupric salt ($\epsilon_{610} \approx 200 \text{ M}^{-1} \text{ cm}^{-1}$ and $A_h = 150 \pm 200 \text{ Gauss}$). For CP, there are conflicting reports in the literature on the ratio of the number of Type I to Type II Cu^{2+} . Andreasson and Vanngard (9) analyzed the 9 GHz EPR spectrum of CP in terms of two ions each of Type I Cu^{2+} and Type II Cu^{2+} . For simulated spectra, the two Type II Cu^{2+} were given slightly different parameters. Veldsema and Van Gelder (10), on the basis of their Nernst plots of titration data, suggested that CP contains one Type I Cu^{2+} and three Type II Cu^{2+} atoms. In the same year, Deinum and Vanngard (11) reported a more detailed analysis of the CP EPR spectra, providing evidence for only one Type II Cu^{2+} ion and for two Type I Cu^{2+} . Finally, Gunnarson *et al.* (12) indicated, after an extensive EPR analysis, the presence of one Type II Cu^{2+} and of two Type I paramagnetic copper ions per

(17)

protein molecule. In addition, they found that the two Type I copper ions exhibit different hyperfine splittings which turn out to be pH-dependent.

As can be seen, the data available in the literature are quite scattered; moreover, the accuracies of the EPR spectroscopic parameters, either from direct measurements or from computer simulation, have never been reported (in most cases "visual" best fits of spectra are shown). In this respect, to get a reliable determination of both the number of the paramagnetic Cu^{2+} ions and of the related EPR parameters (g-values, hyperfine coupling constant, linewidths, relative absorption intensities), we have used a Monte Carlo calculation method to get the best fit of the experimental spectrum of CP at 77 K. The procedure used allowed us to obtain a meaningful evaluation of the spin Hamiltonian parameters which could not be measured directly. Furthermore, Chi-square statistical analysis permitted us to evaluate the accuracy of each parameter involved.

Experimental methods

Human ceruloplasmin was purchased from the Sigma Chem. Co. (Lot:33F-93902). The total copper content of CP, as determined by atomic absorption, was of 106 μg per g of solution. The weight of 1 ml of CP solution was 1.037 g.

Aqueous samples of CP were placed in 4.7 mm i.d. pre-

(18)

cision glass tubes open at both ends, frozen in liquid nitrogen and stored. To record the EPR spectrum, the sample was removed from the glass tube by warming the surface just sufficiently to allow the cylindrical sample to be pushed out of the tube. It was then placed in the E-246 Varian dewar filled with liquid nitrogen. Finally, the dewar tail was inserted in the resonant cavity of the spectrometer. All samples were large enough to fill completely the EPR sensitive volume of the TE_{102} resonant cavity used.

EPR spectra were recorded by an X-band Varian E-109 spectrometer equipped with a variable temperature accessory. A 100 kHz modulation frequency was used for phase-sensitive detection, and the peak-to-peak modulation amplitude never exceeded a value of 5 Gauss to avoid apparent broadening due to over-modulation.

To calculate the experimentally observed g factors, a magnetic field calibration was performed with the Magnion Precision NMR Gaussmeter, Model G-502; the microwave frequency was then determined by the relationship:

$$\nu = g_{\text{DPH}} \beta H/h, \text{ where } g_{\text{DPH}} = 2.0036.$$

An aqueous solution of Cu^{2+} 1mM, in the presence of NaClO_4 0.2 M and HCl 0.02 M, was used to check the sensitivity of the spectrometer from sample to sample and to provide a standardization of the sample EPR intensity.

EPR data acquisition was performed on an HP 86A "personal" computer, through a home-made interface connected to an IEE-488 bus. To run simulation and best fit programs,

the same microcomputer was switched to an intelligent terminal of the mainframe computer through an RS-232-C serial interface and an HP terminal emulator.

Molar concentration of CP was determined spectrophotometrically by using a Mod. 360 Shimadzu spectrometer. By measuring the optical density, OD, at 610 nm and assuming a molar extinction coefficient ϵ , at the same wavelength, of $10,900 \text{ M}^{-1} \text{ cm}^{-1}$ (3) the Beer-Lambert law:

$$c = \frac{OD_{610}}{\epsilon_{610} d} \quad [1]$$

where d is the optical cell path, provided the concentration of the CP molecules in our samples. The concentration of the CP in the lot used throughout all the experiments was determined to be $2.06 \cdot 10^{-4} \text{ M}$.

Data analysis and results

The EPR spectrum of an aqueous solution (pH=6.4) of human CP recorded at 77 K is shown in Fig.1, where the derivative of the paramagnetic resonant susceptibility, χ'' , versus the magnetic field is reported. Since the number of paramagnetic centers contained by the sample is related to the area underlying the EPR absorption spectrum, this number can then be calculated from the second integral of the curve $d^2\chi''/dH^2$ of Fig. 1. By comparing this area to that obtained from a paramagnetic Cu^{2+} standard of known molar concentration,

we calculated a paramagnetic center concentration of $7.0 \cdot 10^{-4} \text{ M}$ for the sample of Fig.1. The total copper content (paramagnetic plus diamagnetic) in CP was calculated to be $1.6 \cdot 10^{-3} \text{ M}$. Then the ratio between these two values indicates that 44% of the total amount of copper contained intrinsically by CP is in a paramagnetic state. This finding is in good agreement with most of the reports dealing with EPR and magnetic susceptibility studies of CP (3). The spectrum of Fig.1 agrees in its essential features with those reported previously (3), which have been interpreted as indicating the presence of two readily distinguishable spectral components, one with a narrow hyperfine splitting (Type I Cu^{2+}) and one with a broader hyperfine splitting (Type II Cu^{2+}). In the two situations the Cu^{2+} ions experience a different symmetry and strength of the crystal field set up by the protein ligands.

In general, most of EPR spectra of copper containing molecules in rigid glass solution can be interpreted in terms of the following spin Hamiltonian (13,14):

$$\mathcal{H} = \beta [H_z g_z S_z + H_x g_x S_x + H_y g_y S_y] + S_z A_z I_z + S_x A_x I_x + S_y A_y I_y \quad [2]$$

where β is the Bohr magneton, $g_{x,y,z}$ and $A_{x,y,z}$ are the g -values and hyperfine splitting components respect to the molecular axes, S is the electron spin ($S=1/2$) and I is the nuclear spin ($I=3/2$). Very often an axial symmetry is displayed by the copper complexes and in this case: $g_x = g_y = g_{\perp}$; $g_z = g_{\parallel}$ and analogously $A_x = A_y = A_{\perp}$; $A_z = A_{\parallel}$.

(21)

Interaction of the unpaired copper electrons with ligand nitrogen nuclei (from the proteic milieu) can give extra hyperfine structure (superhyperfine coupling) and this adds another term to the Hamiltonian:

$$A_{N_z} S_z I_{N_z} + A_{N_x} S_x I_{N_x} + A_{N_y} S_y I_{N_y} \quad [3]$$

where $A_{N_x, y, z}$ are the superhyperfine splittings and I_N is the nitrogen nuclear spin. In the present case no such interaction has been resolved even though it may contribute to the observed linewidths.

To simulate the EPR patterns of CP we have used the following general approach. By solving the orthorhombic spin Hamiltonian [2] to the second order (14,15) the following magnetic field values for the allowed EPR transition are obtained:

$$H = H_0 - \frac{KM_z}{g\beta} - \frac{1}{g^2\beta^2 H_0} \left[\frac{A_z^2 A_y^2}{4B^2} + \frac{A_z^2 B^2}{4K^2} + A_z^2 g_x^2 g_y^2 g_z^2 (A_y^2 - A_x^2)^2 \alpha^2 (1-\alpha^2) \eta^2 \right] \cdot$$

$$\cdot \left[I(I+1) - M_z^2 \right] - \frac{1}{g^2\beta^2 H_0} \left\{ \frac{1-\eta^2}{2K^2 g^2} \left[\frac{g_x^2 g_y^2}{g^2} (A_z^2 - B^2)^2 \eta^2 + \frac{g_x^2 g_y^2}{g^2} (A_x^2 - A_y^2)^2 \alpha^2 (1-\alpha^2) \right] \right\} M_z^2 \quad [4]$$

where:

$$H_0 = \frac{h\nu}{g\beta} \quad [5]$$

(22)

$$g^2 = g_z^2 + (g_x^2 - g_y^2) \eta^2, \quad [6]$$

$$g_1^2 = g_y^2 + (g_x^2 - g_z^2) \alpha^2, \quad [7]$$

$$K^2 g^2 = A_z^2 g_z^2 \eta^2 + B^2 g^2 (1-\eta^2), \quad [8]$$

$$\cancel{B^2 = A_y^2 + (A_x^2 - A_y^2) \alpha^2} \quad g_1^2 B^2 = g_y^2 A_y^2 + (g_x^2 A_x^2 - g_y^2 A_y^2) \alpha^2 \quad [9]$$

and

$$\alpha = \cos \varphi \quad ; \quad \eta = \cos \theta \quad [10]$$

φ being the angle between the projection of the magnetic field in the xy plane and the x axis, while θ is the angle between the magnetic field direction and the z-axis.

For random orientation of the Cu²⁺ ion-bearing molecules (powders or frozen glasses) the absorption $A(H)$ of each hyperfine line is given by:

$$A(H) = (2I+1)^{-1} g_1^2 \sin \theta \left| \frac{d\theta d\varphi}{dH} \right| \quad [11]$$

where

$$g_1^2 = \cancel{g_z^2 \left[\frac{g_x^2 g_y^2}{g^2} + 1 \right]} / 8 = \frac{1}{2} \left[\left(\frac{g_x g_z}{g} \right)^2 + g_y^2 \right] \quad [12]$$

takes into account the variation of the transition probability with the direction of the applied field with

(23)

respect the molecular axis (16).

Expression [11] should be summed over the values of φ and θ for a given H to yield the correct intensity. Then, if the single crystal resonance has the shape $S(H)$, whose first derivative is $S'(H)$ (experimental EPR spectra are commonly displayed as the derivative of the absorption), the derivative of the absorption at a field H_a will be:

$$I(H_a) = \int S'(H_a - H) A(H) dH = (2I+1)^{-1} \int_0^{\pi/2} \int_0^{\pi} S'(H_a - H) g_i^2 \sin\theta d\theta d\varphi \quad [13]$$

the total derivative of the absorption being obtained by a summation over all the hyperfine lines (with different M_x).

We have used Gaussian line-shapes for which:

$$S'(H) = 2\pi^{-1/2} \gamma^{-3} H e^{-\left(\frac{H}{\gamma}\right)^2} \quad \text{with} \quad \gamma = 2^{-1/2} \Delta H \quad [14]$$

ΔH being the separation between points of maximum and minimum slope.

The expression used were programmed in Fortran 77 for a Prime 350/1 computer. Programs were run in double precision, and integration in θ was carried out with the Simpson method on 80 points, while integration in φ was performed for 10 points. Under these condition no "computer noise" was observed.

The computer-synthesized EPR spectra were used to fit the experimental spectrum obtained at 77 K from the CP aqueous solution of Fig.1.

According to the method of least-squares, the best fit is obtained by minimizing the functions:

(24)

$$F(p) = \sum_{i=1}^N \left[I^{exp}(H_i) - I^{th}(H_i, p) \right]^2 \quad [15]$$

with respect to set of parameters p . I^{exp} is the derivative of the total absorption sampled at $N=250$ discrete points of the field. $I^{th}(H, p)$ is the model function which is non-linear (transcendental) in its parameters p . The parameters taken into account were the g -values (g_x, g_y, g_z), the hyperfine couplings (A_x, A_y, A_z) and the line widths ($\Delta H_x, \Delta H_y, \Delta H_z$) of each type of Cu^{2+} paramagnetic center. To fit the composite experimental spectrum of Fig.1, the theoretical lineshape was considered as a sum of the type:

$$I^{th}(H, p) = \sum_{i=1}^M \alpha_i I_i^{th}(H, p_i) \quad [16]$$

where the α_i are the molar fractions, the I_i^{th} are the normalized theoretical spectra of the n different Cu^{2+} paramagnetic sites present in the CP molecule and the p_i are now the subsets of parameters each related to these theoretical spectra.

In order to be efficient, the least-squares method requires that the starting parameters p^0 approach the values p^* of the minimum of $F(p)$ and in this case the values of the α_i can be determined. Wrong guesses normally either do not lead to convergence or may give rise to local minima. When more than one Cu^{2+} complex (with different EPR characteristic) is presents, the EPR spectra are too complicated to make a reliable estimate of all the parameters. Very often, the only reasonable assumption which can be made is

one about their possible range of variation. In this respect, the Monte Carlo method allows us to deal with the problem of minimizing the function [15] in a realistic way, so that meaningful evaluation of the p parameters can be obtained. On the other hand, a careful analysis of the experimental spectra and certain experimental results taken from the literature can give us a determination of the number (n) of different paramagnetic centers appearing in [16] together with determination of some of the EPR parameters. If we look at Fig.1, the EPR line situated at about 2640 Gauss is the low field hyperfine component ($M_x = -3/2$) in the parallel region of the spectrum, arising from Type II Cu²⁺ ions coordinated to the protein in a tetragonal symmetry (4,17). Since this component is relatively isolated, it is possible to measure the EPR linewidth $\Delta H_{||}$ relative to this type of copper. In all the sample at pH=6.4 we found $\Delta H_{||} = 67 \pm 2$ Gauss. Moreover, the total EPR intensity due to Type II Cu²⁺ centers can be calculated by measuring the area under this hyperfine line in the derivative spectrum (18,19). By using this procedure on different samples from the same lot of CP and comparing the results with our Cu²⁺ standard we calculated a Type II Cu²⁺ concentration of $2.9 \cdot 10^{-4}$ M. This value means that about 41% of the total content of paramagnetic copper is of Type II.

As regards the Type I Cu²⁺ ions, a careful analysis of the EPR spectrum of CP at low temperature as a function of pH reveals the presence of two different type (Type Ia and Type Ib) of such paramagnetic centers (12). A near tetrahe-

dral geometry has been indicated for Type I Cu²⁺ ions (3,4). Small conformational changes induced by pH variations could modulate the symmetry and/or the strength of the crystal field sensed by these ions. In addition, the two blue centers have been shown to possess different redox potentials (3). Indeed, we observed such a variation in the CP EPR spectrum when the pH was varied (not shown).

In conclusion, the above considerations allow us to break down expression [16] into the sum of three terms ($n=3$) each referring to the normalized theoretical spectrum characterized by a different set of spin Hamiltonian parameters:

$$I^{th}(H, P) = \alpha_1 I_{Type II}^{th}(H, P_1) + \alpha_2 I_{Type Ia}^{th}(H, P_2) + \alpha_3 I_{Type Ib}^{th}(H, P_3) \quad [17]$$

To run Monte Carlo simulation, we allowed each EPR parameter to vary over a wide range, consistent both with that estimated from the experimental spectra and with that reported in literature for each Cu²⁺ type (3,4,9,11,12,17).

Best fit of I^{exp} was obtained after running more than 100,000 histories. The results are summarized in Fig.2 and Table I. The theoretical spectrum arising from the best fit is shown in Fig.2b where it is compared with the experimental spectrum (Fig.2a). The theoretical spectrum consists of the sum of three different spectra due two Type II (Fig. 2c), Type Ib (d) and Type Ia (e) Cu²⁺ ions.

In Table I the EPR parameters p^* obtained for each type of paramagnetic copper, their standard deviations and their molar fractions are listed. Standard deviations of the pa-

parameters were calculated by the Chi-square method. The numerical value obtained for the expression:

$$\chi^2 = \sum_{i=1}^N \left[\frac{I^{exp}(H_i) - I^{th}(H_i, p^*)}{\sigma_i} \right]^2 \quad [18]$$

was 582, and the g_i were calculated after repeated runs of the same experimental spectrum through the on line data acquisition system.

Discussion

The Monte Carlo procedure has never, to the best of our knowledge, been used to fit experimental EPR spectra of metallo proteins. The method has the great advantage of dealing realistically with a minimization problem when the simultaneous variation, over a wide range, of several non-linear parameters has to be taken into account. Furthermore the method allows us to scan the local minima and thus avoid wrong guesses about the starting parameters.

In our case, the method permitted us, after more than 35 days of calculation time, to obtain a good fit of the experimental data.

As can be seen from Table I, the g_i of each copper type was calculated with the highest accuracies. In this respect, it should be noted that slight variations around these g_i values contributed significantly to expression [18] even though the highest σ_i values were obtained exactly in this region

of the spectrum. The lowest accuracy was obtained for the A_i of Type Ia Cu^{2+} , owing to the smooth variation of expression [18] as a function of this parameter.

The molar fractions obtained as coefficients of the normalized spectra of the best fit are very close to those calculated from the experimental spectrum. Type II copper accounts for about 41% of the total paramagnetic copper; the quantities of Type Ia and Type Ib Cu^{2+} ions per molecule of CP are equal one to the other. This means that each molecule of CP contains 1 Type Ia, 1 Type Ib and 1.4 Type II Cu^{2+} ions. The non-integral value obtained for Type II copper is consistent with the hypothesis that the CP molecule, depending on its preparation, can randomly pick up a Type II Cu^{2+} ion which is not part of the native enzyme (8). Effectively we observed that, when the spectrum of CP is recorded at pH=9 a small shoulder of the 2640 Gauss EPR line appears at low fields (not shown).

In conclusion, we reported a calculation method which, more generally, may provide a reliable determination of the spin Hamiltonian parameters relative to different paramagnetic entities in a diamagnetic matrix and whose EPR spectra display an extensive overlap. In particular, selectively-induced changes in the different paramagnetic center microenvironments, with subsequent partial variations in the overall EPR pattern, can be reasonably attributed.

Acknowledgements

Part of this work has been supported by a CNR and MPI grants. Thanks are due to Prof. F.Sacchetti for many stimulating discussions and to Mr. P.Tancini for invaluable help in interfacing the EPR spectrometer to the personal computer. Thanks are also due to Prof. D.Boothman for his reading of the manuscript.

References

- (1) M.Bomba, A.Camagna, S.Cannistraro, P.L.Indovina and P.Samoggia: *Physiol. Chem. Physics*, 9, 175 (1977); and references cited therein.
- (2) S.Cannistraro, F.Ianzini and P.L.Indovina: *Studia Biophysica*, 86, 163 (1981).
- (3) J.A.Fee: *Structure and Bonding*, 23, 1 (1975); and references cited therein.
- (4) A.S.Brill: "Transition Metals in Biochemistry" (Springer Verlag, New York, 1977).
- (5) S.Onori, A.Rosati and S.Cannistraro: *Physiol. Chem. Physics*, 13, 439 (1981).
- (6) G.Biaquinta, C.Di Mauro, S.Onori, S.Cannistraro: *Biophys. J.* (1984) submitted for publication.
- (7) S.Cannistraro and F.Sacchetti: *Physics Lett.A*, (1984) in press.
- (8) L.Ryden and I.Bjork: *Biochemistry*, 15, 3411 (1976).
- (9) L.E.Andreasson and T.Vanngard: *Biochim. Biophys. Acta*, 200, 247 (1970).
- (10) A.Veldsema and B.F.Van Gelder: *Biochim. Biophys. Acta*, 293, 322 (1973).
- (11) J.Deinum and T.Vanngard: *Biochim. Biophys. Acta*, 310, 321 (1973).
- (12) P.Gunnarsson, U.Nylen and G.Petterson: *Eur. J. Biochem.*, 37, 47 (1973).
- (13) B.R.McGarvey: "Transition Metal Chemistry", edited by R.L.Carlin (M.Dekker Inc., N.Y., 1966) vol. 3 p. 89.
- (14) A.Abragam and B.Bleaney: "Electron Paramagnetic Resonance of Transition Ions", (Oxford University Press, 1970).
- (15) R.A.Breslow and F.J.Owens: *Chem. Phys. Lett.*, 16, 20 (1972).
- (16) B.Bleaney: *Proc. Phys. Soc. A*, 75, 621 (1960).
- (17) J.H.Dawson, D.M.Dooley and H.B.Gray: *Proc. Natl. Acad. Sci. USA*, 75, 4078 (1978).
- (18) T.Vanngard: "Magnetic Resonance in Biological System", (Pergamon Press, Oxford, 1967) p.213.
- (19) T.Vanngard and R.Aasa: *J. Magnetic Res.* 19, 309 (1975)

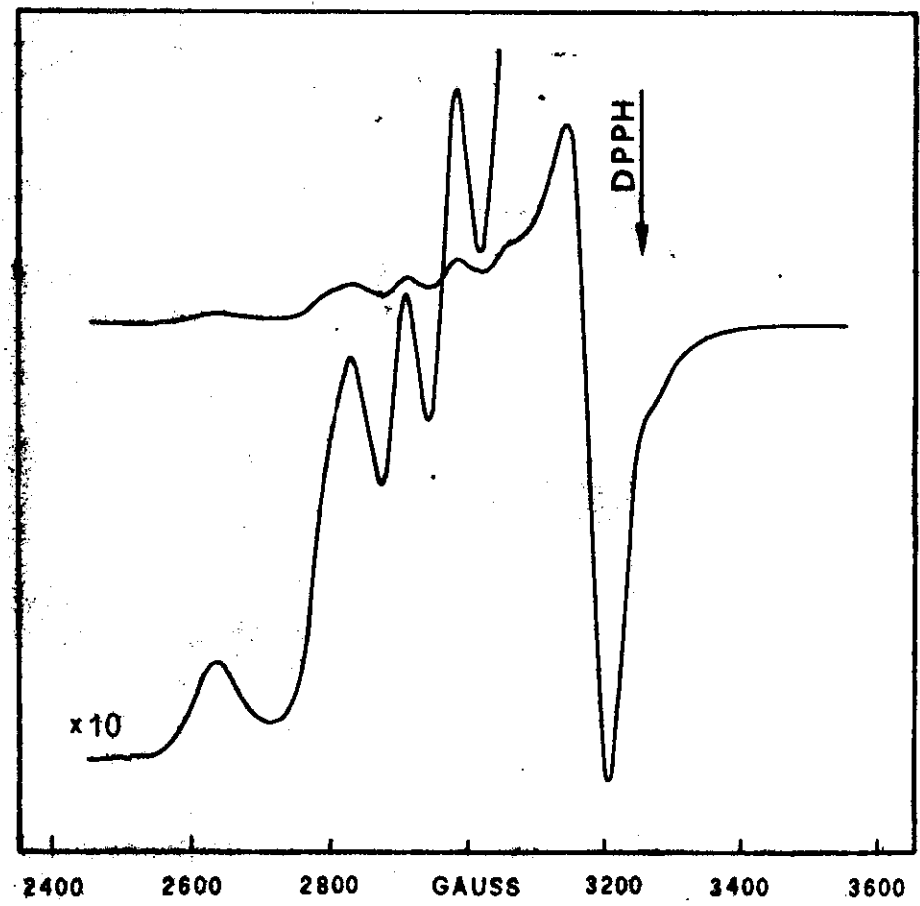
Legends of figures

Fig.1 EPR spectrum of CP recorded at 77 K. $d\chi/dH$ is reported on the vertical axis. Low field part of spectrum is shown at a ten-fold higher gain. Microwave power level: 20 mW. Magnetic field sweep rate: 2000 Gauss in 8 min. Time constant: 0.5 s. Modulation amplitude: 5 Gauss

Fig.2 Experimental (a) and computer synthesized (b) EPR spectra of human CP. Experimental spectrum was recorded as in Fig.1. Computer simulated spectrum was the result of the Monte Carlo best fit. It was the sum of three components: a Type II (c), a Type Ib (d) and a Type Ia (e). Their EPR parameters are reported in Table I.

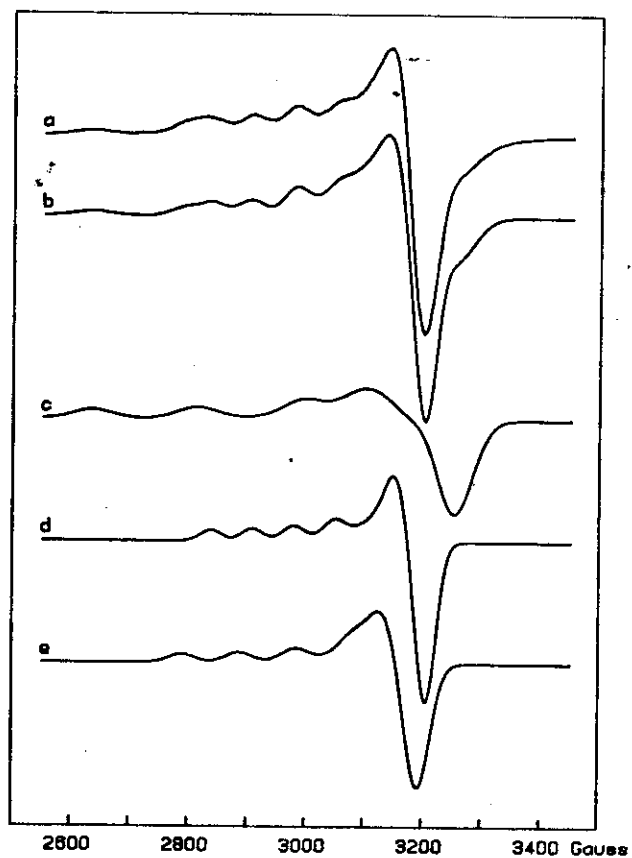
G. Giuglioulli *et al*

FIG 1



(33)

Fig. 2



(34)

Table I. EPR parameters and molar fractions (\pm standard deviation) related to the three spectroscopically different CF Cu^{2+} ions, as calculated by the best fit of the experimental data.

Parameter	Type II	Type Ia	Type Ib
$g_{\parallel} = g_{\perp}$	2.2468 ± 0.0014	2.2227 ± 0.0013	2.2159 ± 0.0011
$g_{\parallel} = g_{\perp} = g_{\text{iso}}$	2.0596 ± 0.0007	2.0632 ± 0.0005	2.0489 ± 0.0002
$A_{\parallel} = A_{\perp}$	177.8 ± 1.5	96.1 ± 1.3	70.1 ± 0.7
$A_{\parallel} = A_{\perp} = A_{\text{iso}}$	23.4 ± 1.5	9.6 ± 5.0	10.8 ± 0.5
$\Delta H_{\parallel} = \Delta H_{\perp} = \Delta H_{\text{iso}} = \Delta H$	65.7 ± 2.0	43.8 ± 1.2	35.3 ± 0.6
Molar fraction	$\alpha_2 = 0.39 \pm 0.01$	$\alpha_1 = 0.27 \pm 0.05$	$\alpha_3 = 0.29 \pm 0.01$

Riassunto

La ceruloplasmina umana contiene diversi ioni Cu^{2+} alcuni dei quali sono paramagnetici. Di questi ne sono stati ipotizzati due tipi (Tipo I e Tipo II), ognuno di essi con caratteristiche spettroscopiche diverse. Tuttavia esistono nei lavori precedenti discordanze sia sul numero di ioni Cu^{2+} che sui loro parametri EPR.

Si è usato il metodo Monte Carlo per ottenere il best fit dello spettro EPR della ceruloplasmina. Lo spettro simulato è risultato la somma di tre spettri, 2 di Tipo I (Tipo Ia e Tipo Ib) e 1 di Tipo II. Sono stati così determinati i parametri relativi all'Hamiltoniana di spin del sistema e le loro deviazioni standard.

MOLECULAR STRUCTURE AND DYNAMICS OF HUMAN CERULOPLASMIN

I would like to present some results concerning a human serum protein, Ceruloplasmin (CP), as obtained by the spin labeling technique and by Small Angle Neutron Scattering (SANS).

Ceruloplasmin is a copper containing protein showing many interesting biophysical features. Its biological role is highly debated even if some hypothesis have been put forward (ferroxidase activity, iron mobilization, copper transport, etc...). In any case it behaves as an oxidase enzyme, the electrons taken to the substrate being at last released to molecular oxygen through an interesting electron transfer mechanism (tunneling?) in which all the spectroscopically different copper ions seem to be involved.

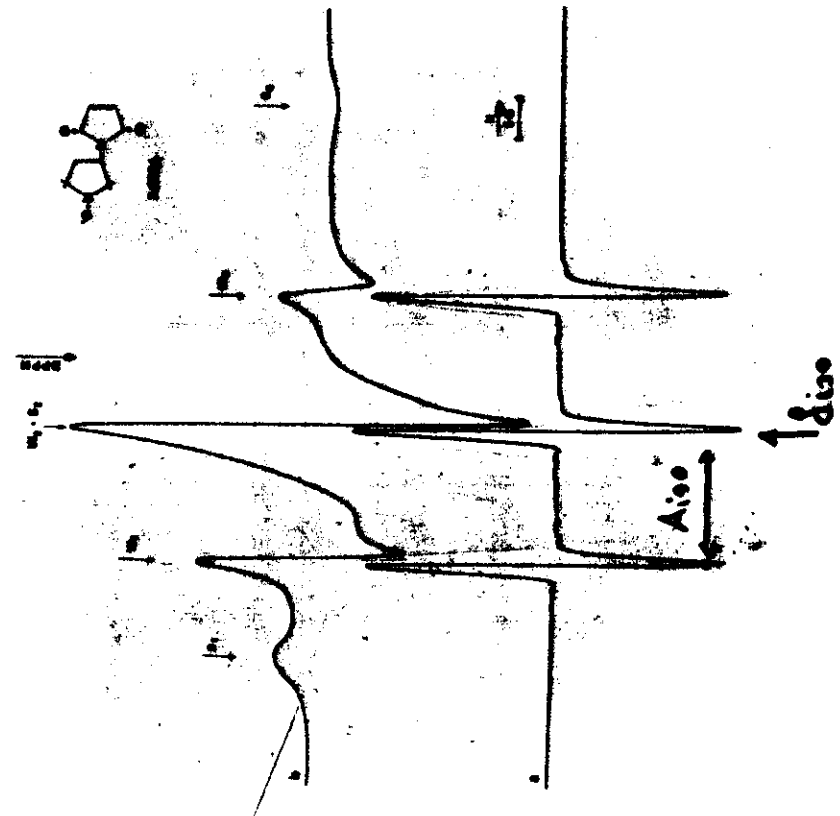
Moreover CP is involved in many pathological stresses (cancer, myocardial infarction, etc...)

Finally it seems that CP undergoes an high temperature "excitonic" superconductive transition when stored in the frozen state.

Spin labeling technique is a very useful spectroscopic approach which may provide information about the rotational dynamics of biomolecules, on the conformational changes to which biomolecules may undergo and on the molecular interactions with suitable substrates.

Spin labeling consists in the covalent binding of a stable free radical (commonly a nitroxide molecule bearing an unpaired electron) to the protein and in the analysis of the Electron Spin Resonance spectra obtained (unbound spin label molecules must be removed!).

- ESR spectra -



The ESR spectra of a nitroxide radical (spin, $S = \frac{1}{2}$) can be interpreted in terms of the spin Hamiltonian:

$$\mathcal{H} = \underbrace{\beta \vec{H} \cdot \vec{g} \cdot \vec{S}}_{\text{Zeeman term}} + \underbrace{\vec{I} \cdot \vec{A} \cdot \vec{S}}_{\text{hyperfine term}} \quad \begin{array}{l} S = \frac{1}{2} \\ I = 1 (^{14}\text{N}) \end{array}$$

The success and importance of the spin labeling method of studying the structure and dynamics of macromolecules is based on the fact that \vec{g} and \vec{A} tensors are anisotropic, making the ESR spectra critically dependent on the orientation of the spin label.

When the spin labels are allowed to tumble rapidly in an isotropic way the spin Hamiltonian becomes time-dependent:

$$\mathcal{H} = \mathcal{H}_0 + \mathcal{H}_1(t) = \underbrace{\beta g_{iso} \vec{H} \cdot \vec{S} + A_{iso} \vec{I} \cdot \vec{S}}_{\text{isotropic part}} + \underbrace{\beta \vec{H} (\vec{g} - g_{iso}) \cdot \vec{S} + \vec{I} (\vec{A} - A_{iso}) \cdot \vec{S}}_{\text{anisotropic part}}$$

where the isotropic values, g_{iso} and A_{iso} , of the tensors \vec{g} and \vec{A} are:

$$g_{iso} = \frac{1}{3}(g_{xx} + g_{yy} + g_{zz}) \quad A_{iso} = \frac{1}{3}(A_{xx} + A_{yy} + A_{zz})$$

If the (molecular motion is fast enough:

$|\mathcal{H}_1(t)|/\mathcal{H}_0 \leq 1$; $\mathcal{H}_1(t)$ can be treated as a time-dependent perturbation and gives rise to line broadening (induction of transitions between electronic and nuclear spin states and modulation of energy levels).

The line positions can be calculated by \mathcal{H}_0 which yields a three line spectrum (with splitting A_{iso} and centered at g_{iso}) [FIG].

If the motion is very fast ($\tau_c \leq 10^{-10}$ s) the spectrum will consist of three sharp lines of equal height. As the motion becomes progressively slower (i.e. by increasing the viscosity of the medium or by branching the spin label to a bigger molecule) there is a differential broadening of the lines, while the line positions remain constant [W in FIG].

For values of $\tau_c > 5 \cdot 10^{-9}$ s (slow motional region) a distortion of the line positions and line shape is observed and a breakdown of the time-dependent perturbation.

(41)

approach occurs. [S in FIG]

Paramagnetic spin labels tumbling in both motional regions contribute to the ESR spectrum of the spin labeled CP (W, weakly immobilized; S strongly immobilized)

How is it possible to extract useful information from the ESR spectra?

Going back to the fast motional situation, since the spin label is tumbling randomly, $H_1(t)$ is a random function of time and the autocorrelation function of $H_1(t)$:

$$G(\tau) = \overline{H_1(t) H_1(t+\tau)}$$

measures the persistence of the fluctuations in the system. It depends on the particular model adopted for molecular reorientation. Brownian rotational diffusion is generally a good description for the motional behaviour of macromolecules such as proteins in solution. In this case:

$$G(\tau) = \overline{H_1^2(t)} e^{-\tau/\tau_c}$$

If the spin label is approximated by a rigid sphere of radius R rotating in a medium of viscosity η , then the Debye-Stokes-Einstein

(42)

relationship yields:

$$\tau_c = \frac{4\pi}{3} \frac{\eta R^3}{kT}$$

The relaxation processes induced by $H_1(t)$ are determined by the spectral density $J(\omega)$ which is the Fourier transform of $G(\tau)$ which takes in our case the form:

$$J(\omega) = \int_{-\infty}^{+\infty} G(\tau) e^{i\omega\tau} d\tau = \frac{2\tau_c}{1+\omega^2\tau_c^2} \overline{H_1^2(t)}$$

An exact derivation of the line width of the ESR absorptions in terms of $J(\omega)$ provides:

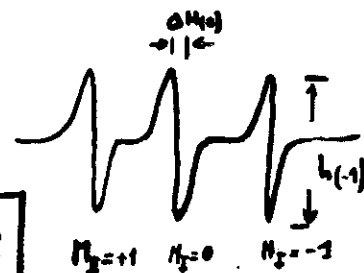
$$\Delta H(H_Z) = A + B M_Z + C M_Z^2$$

ΔH = peak-to-peak linewidth

For Lorentzian line shapes:

$$B = \frac{1}{2} \Delta H(0) \left[\sqrt{\frac{h(0)}{h(+1)}} - \sqrt{\frac{h(0)}{h(-1)}} \right]$$

$$C = \frac{1}{2} \Delta H(0) \left[\sqrt{\frac{h(0)}{h(+1)}} + \sqrt{\frac{h(0)}{h(-1)}} - 2 \right]$$



(43)

Taking into account the explicit expression for B and C it can be obtained:

$$\tau_c = -1.22 \cdot 10^{-9} B$$

$$\tau_c = 1.19 \cdot 10^{-9} C$$

For 3MAL-CP we measured: $\tau_c = 1.96 \cdot 10^{-9}$

$$\tau_c = 2.10 \cdot 10^{-9}$$

The labels (selective for SH groups) are bound to the CP at sites which allow the labels to retain a large degree of rotational freedom with respect to the tertiary structure of the protein (polar medium, surface).

These kind of ^{bound} spin labels are very sensitive reporters of the microenvironment: even a slight change in their degree of rotational freedom, as induced by a conformational variation of the macromolecule or subsequent to a molecular interaction with another biosystem, would immediately be registered as a change in the ESR line width and heights and hence in τ_c . Experiments

The calculation of the correlation time of the bound spin labels which give rise to the asymmetric critical anisotropic signal (S, powder like spectrum)

(44)

is more complicated. Since $FE_s(t)$ does not fluctuate rapidly enough, the perturbation approach is no longer valid. In this case it is necessary to simulate the spectra, both position and line width depending on τ_c .

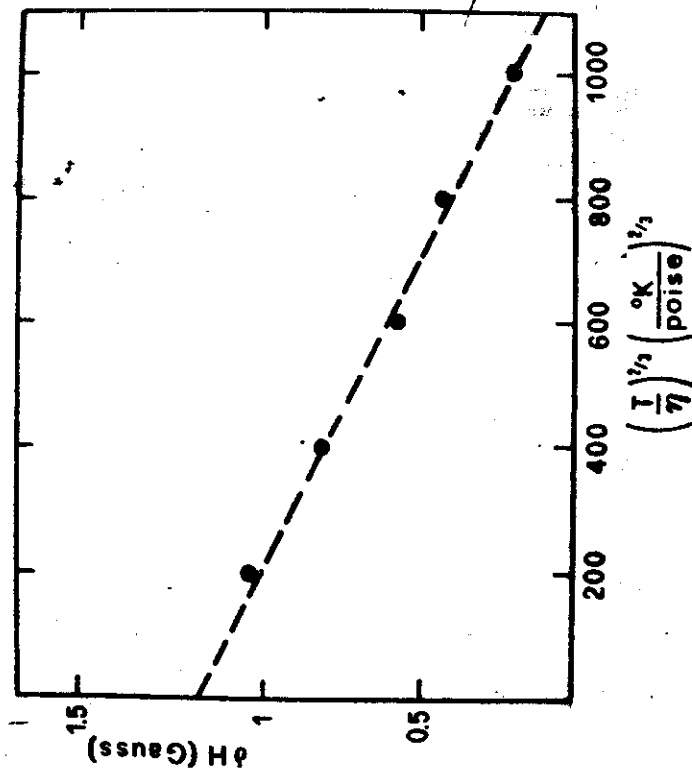
Two approaches have been developed.

The simpler one takes into account the solution of the Bloch equations coupled to a diffusion term:

$$\frac{d\vec{H}}{dt} = \gamma \vec{H} \wedge \vec{H} - \frac{1}{T_2} (\mu \vec{i} + \nu \vec{j}) - \frac{1}{T_1} (H_z - H_0) \vec{k} + D \nabla^2 \vec{H}$$

A numerical solution of this equation leads to express quantitatively a dependence of the resonance positions of the outer hyperfine extrema (S_1 and S_3 in our case) on rotational motion. In practice, the correlation time of the strongly immobilized spin labels can be determined by measuring the high field (or low field) hyperfine component position as function of viscosity η and extrapolating to infinite viscosity (Fig. 107)

(45)



(46)

The extrapolated shift $\delta H = 1.26$

corresponds to a τ_c of 10^{-7} s

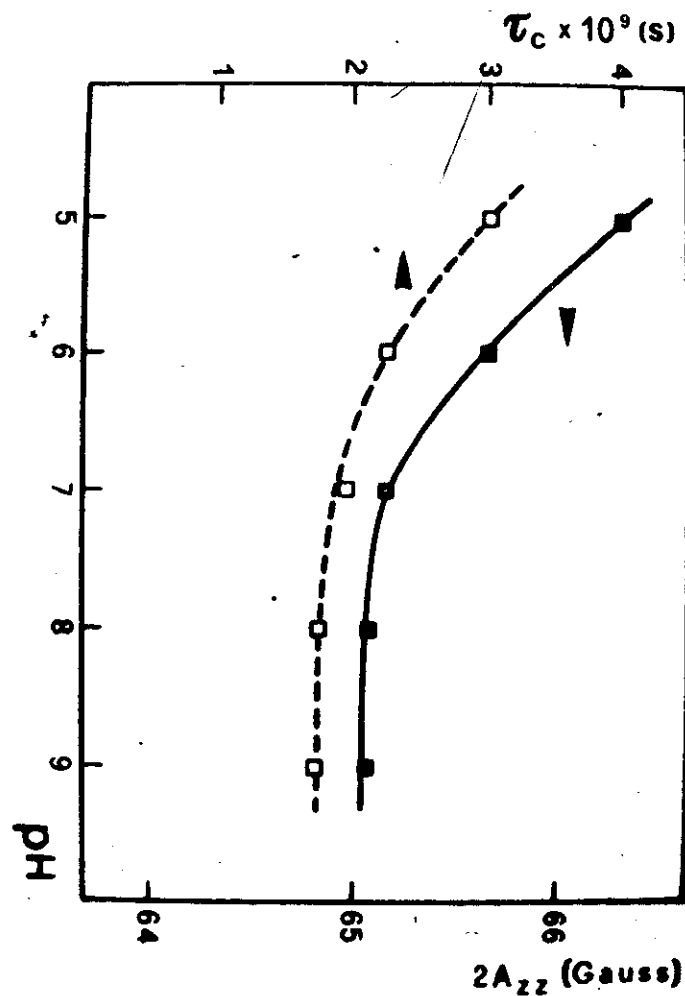
Now since these bound spin labels have no residual rotational motion with respect to the protein tertiary structure, this correlation time contains information about the tumbling of the whole biomolecule. Then under the assumption of a spherical shape for CP, a reliable estimate of its radius R can be obtained from the Stokes-Einstein relationship:

$$R = \left(\frac{3kT\tau_c}{4\pi\eta} \right)^{1/3} = 39.5 \pm 2 \text{ \AA}$$

- Other experiments (pH, int. with function)
FIG 121

Some criticism could be made: a rigid sphere model has been assumed for the protein; actually proteins in solution may undergo extensive interaction with solvent and in some cases a hydrated layer should be considered. Consequently, the microviscosity at protein surface may fluctuate significantly

(47)



(48)

and differ from bulk viscosity; this fact may affect the value of R obtained through the Stokes Einstein relationship.

To get an independent estimate of this value we performed some SANS measurements on CP solutions. The results:

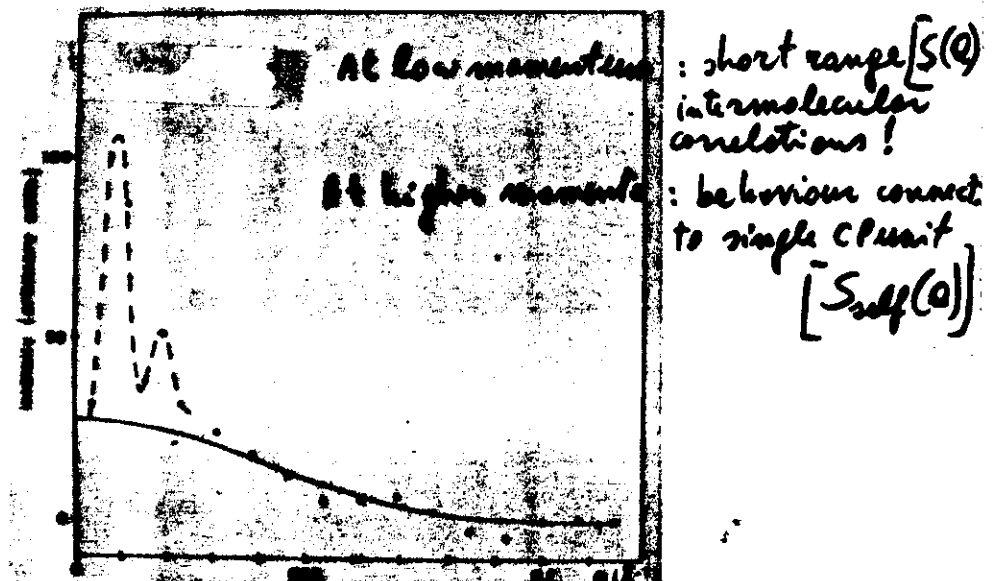


Fig. 1. SANS intensity versus Q (dotted line). The dashed line is only guide to the eye. The full line curve is the fitted $S_{self}(Q)$ (see text).

The total scattered intensity is proportional:

$$I(Q) \propto S_{self}(Q) S(Q)$$

By a fitting of $S_{self}(Q)$, in a form appropriate to spherical scattering units we obtained

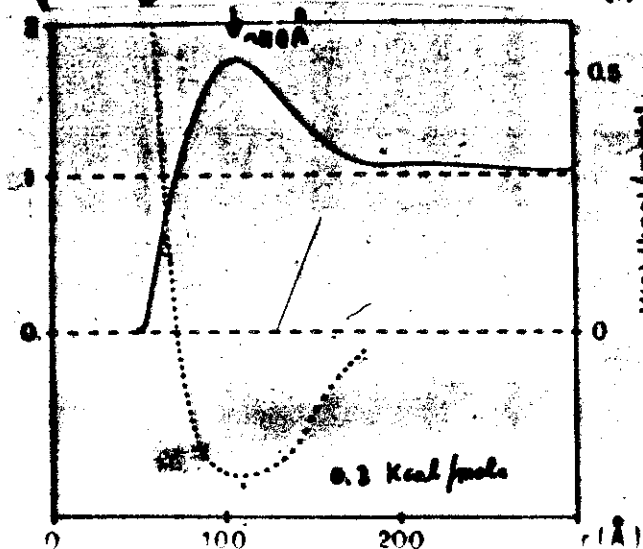
a radius $R = 42.6 \pm 3 \text{ \AA}$. in good agreement with the previous one.

Moreover, by using the self scattered term we deduced $S(Q)$. A two unit correlation function can be derived from $S(Q)$:

$$g(r) = 1 + (2\pi n r)^{-1} \int_0^\infty [S(Q) - 1] \sin(Qr) Q dQ$$

$n = \text{density CP}$

As is well known $4\pi n r^2 g(r) dr$ is the probability of having one unit at a distance r , another unit being at the origin. \downarrow Since $nR^3 \ll 1$; the correlation function is reasonably approx



by:
 $g(r) = e^{-[V(r)/kT]}$
 $V(r)$: a two unit potential

Conclusions

SMALL ANGLE NEUTRON SCATTERING AND SPIN LABELING OF HUMAN CERULOPLASMIN

Salvatore CANNISTRARO and Francesco SACCHETTI

Gruppo di Biologia Molecolare, Dipartimento di Fisica dell'Università, I-06100 Perugia, Italy

Received 16 January 1984

Small angle neutron scattering evidence of intermolecular correlations between ceruloplasmin units in aqueous medium is provided. By the same technique, the radius of gyration of the globular biomolecule has been calculated to be $33 \pm 3 \text{ \AA}$. This value was found to agree very well with that measured by the authors with a spin labeling approach.

Ceruloplasmin (CP) is a paramagnetic copper protein which shows many interesting spectroscopic and biophysical aspects [1] and perhaps a superconducting behaviour at high temperature [2].

The detailed structure of crystallized CP has not been determined even if some partial results have appeared in the literature [3]. Accordingly, a molecular weight, M , of 132,000 daltons and a partial specific volume, \bar{v} , of $0.7149 \text{ cm}^3 \text{ g}^{-1}$ have been obtained for the globular protein. Then, assuming a spherical molecular shape of radius R , the radius of gyration, R_g , can be calculated as follows:

$$R_g = \left(\int_0^R r^2 (r^2 dr) \right) \left(\int_0^R r^2 dr \right)^{-1} = (3/5)^{1/2} R = (3/5)^{1/2} (3M\bar{v}/4\pi N)^{1/3} \approx 26 \text{ \AA}, \quad (1)$$

where N is Avogadro's number.

To get an independent estimate of this parameter and in order to check some spin labeling results concerning the molecular dynamics of CP [4], we have performed some small angle neutron scattering (SANS) measurements on the protein.

In the course of such a study we surprisingly found some well-defined intensity peaks in the small momentum region (0.01 \AA^{-1}). These peaks have been interpreted in terms of intermolecular correlations existing in the aqueous solutions of CP units.

SANS measurements were performed at 20°C on the two crystal diffractometer [5] at the 1 MW TRIGA

reactor, Casaccia. Two almost perfect germanium crystals with the (220) reflection in symmetrical transmission were employed, with an angular resolution of 5×10^{-3} degrees. The sample chamber was glass, wall thickness 0.2 mm , and the specimen was 2 mm thick. CP (purchased from Sigma Chem.) was dissolved in an aqueous solution at a concentration of 0.1 mM . SANS measurements were made by scanning the scattering angle, 2θ , in steps of 0.5° . A typical scan contained 50 steps and required 3 h running time. The background was routinely subtracted from the scattered intensity.

The SANS intensity was plotted as a function of the exchanged momentum and the pattern obtained is shown in fig. 1. The plot exhibits a number of maxima and minima implying that there must be some order present in the aqueous solution of CP. Apart from an obvious scale factor, the general trend closely resembles the X-ray scattering from a simple liquid [6]. Accordingly, two regions can be considered in the plot. In the low momentum region ($Q < 0.02 \text{ \AA}^{-1}$) the rather sharp peaks can be attributed to short range intermolecular correlations, while the smooth behaviour observed at higher momenta ($Q > 0.04 \text{ \AA}^{-1}$) is connected to the single CP unit. In other words, the present data can be interpreted in terms of both a single scattering factor, $S_{\text{scat}}(Q)$, and a structure factor, $S(Q)$, describing the intermolecular correlation. The total scattered intensity is then proportional to:

$$I(Q) \propto S_{\text{scat}}(Q)S(Q). \quad (2)$$

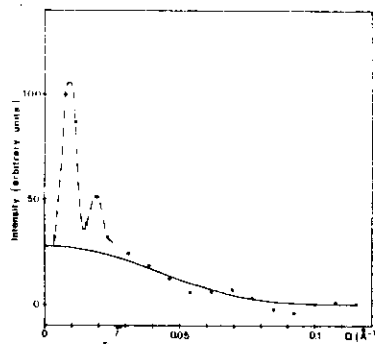


Fig. 1. SANS intensity versus exchanged momentum (dotted line). The dashed line is solely guide to the eyes. The full line curve is the fitted $S_{\text{self}}(Q)$ (see text).

A two unit correlation function can be derived from $S(Q)$:

$$g(r) = 1 + (2\pi^2 n r)^{-1} \int_0^\infty \{S(Q) - 1\} \sin(Qr) Q dQ, \quad (3)$$

n being the number density of the CP units. As is well known, $4\pi n r^2 g(r) dr$ is the probability of having one unit at a distance r , another unit being at the origin.

By assuming a spherical shape for the CP units, we fitted $S_{\text{self}}(Q)$, in a form appropriate to spherical uniform scattering units, to the experimental data in the range $0.05 \text{ Å}^{-1} < Q < 0.1 \text{ Å}^{-1}$ obtaining a gyration radius $R_g = 33 \pm 3 \text{ Å}$ and hence $R = 42.6 \pm 3 \text{ Å}$. By using the obtained self scattering term, we deduced $S(Q)$ and hence $g(r)$. Looking at the full line curve of fig. 2, we observe that $g(r)$ shows a well-defined maximum at $r = 110 \text{ Å}$, no other appreciable peaks being present. It should be remarked that the average distance between the CP units, at the density used in the present study, was estimated to be about 290 Å : a value which is about 7 times larger than the radius estimated for the CP molecules. Because of the very low density at which our system is dissolved in the aqueous medium ($nR^3 = 0.0047$), the correlation function is reasonably ap-

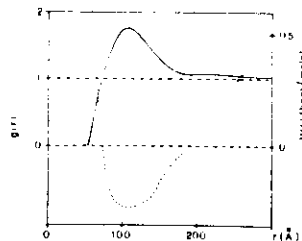


Fig. 2. Two body correlation function versus distance (full curve) and two body potential (dotted curve).

proximated by the following expression (7):

$$g(r) = \exp[-V(r)/kT], \quad (4)$$

where $V(r)$ is the two unit potential. The plot of $V(r)$ is also shown in fig. 2 (dotted curve). As can be seen, an attractive potential appears to be operating between the CP units. This potential shows a minimum of about $0.3 \text{ kcal per mole}$ around 110 Å .

As concerns the radius of gyration, the value obtained by us seems somewhat higher than that deduced by eq. (1). We thus tried to check this value by an independent physical method. By a spin labeling approach we determined the rotation correlation time, τ_c , of a nitroxide radical covalently bound to CP, without rotation motion relative to the tertiary structure of the protein [4]. The method [8] assumes isotropic brownian diffusion of molecules and allows one, after solution of the Bloch equations coupled with a diffusion term, to determine τ_c from the shifts which lines S_1 and S_3 of fig. 3 undergo upon a change of the viscosity. The correlation time is connected, through Einstein and Debye relations, with the radius of the molecule, the viscosity, η , of the medium and the temperature, as follows (9):

$$\tau_c = 4\pi\eta R^3/3kT. \quad (5)$$

By this method, we have calculated a correlation time of 10^{-7} s , at 293 K . Then, using a value of $\eta = 0.0128 \text{ poise}$ (measured for the CP solution by an Ostwald viscosimeter), relation (5) gives $R = 39.5 \pm 2 \text{ Å}$.

This value is in good agreement with that obtained by SANS measurement, under the same assumption

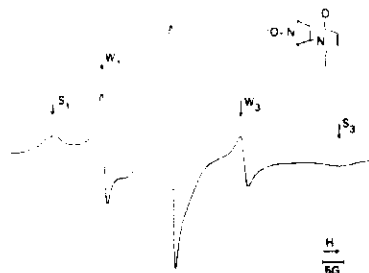


Fig. 3. Electron spin resonance spectrum of CP, spin labeled with the 3 MAL free radical (chemical formula in the insert). The overall spectrum is a composite of two triples of which S_1 , S_3 and W_1 , W_3 are the respective outer components. Triplet hyperfine structure arises from the interaction of the unpaired electron with ^{14}N nucleus. W_1 , W_3 are referred to a triplet spectrum due to bound spin labels, weakly immobilized with respect to the protein. On the other hand S_1 and S_3 belong to a triplet structure arising from bound labels with no residual rotational motion with respect to the protein (i.e. strongly immobilized).

of a spherical shape for CP.

The present results may lead to many speculative discussion about the possible biological role played by the correlation existing between the CP molecules and about the intermolecular forces governing the attractive interaction which seems to be operating within the biomolecules. At present however, we are not able to estimate the biophysical implications of such a correlation. In this connection, it is worth noting that a

similar correlation, but at much larger range, has been observed in aqueous solutions of another biomolecule, bovine serum albumin [10]. In these papers, the authors suggest that the biomolecules aggregate, under an attractive interaction, giving rise to regions (clusters) where the local concentration is higher than the average value.

This study was carried out under an ENEA-CNR agreement and was partly supported by CNR and MPI Grants.

References

- [1] J.A. Fee, Structure and bonding, Vol. 23 (Springer, Berlin, 1975) p.1.
- [2] G. Giacomini, C. Di Mauro, S. Onori and S. Cannistraro, submitted to Biophys. J. (1983).
- [3] B. Magdoff-Fairchild, F.M. Lowell and B.W. Low, J. Biol. Chem. 244 (1969) 3497.
- [4] F. Ianzini, P.L. Indovina and S. Cannistraro, Proc. 8th ISMAR Conf. (Chicago, 22-26 August 1983); S. Cannistraro and P.L. Indovina, to be published.
- [5] C.S. Schneider and C.G. Shull, Phys. Rev. B3 (1971) 830.
- [6] R.W. James, The optical principles of the diffraction of X-rays (Bell, London, 1958).
- [7] J.M. Ziman, Models of disorder (Cambridge Univ. Press, London, 1979).
- [8] R.C. McCalley, F.J. Shimshick and H.M. McConnell, Chem. Phys. Lett. 13 (1972) 115.
- [9] A. Carrington and A.D. McLachlan, Introduction to magnetic resonance (Harper, New York, 1969).
- [10] R. Giordano, F. Mallamace and F. Wanderlingh, Nuovo Cimento 2D (1983) 1272, and references therein.

MOLECULAR DYNAMICS AND INTERACTIONS OF HUMAN CERULOPLASMIN: A SPIN LABELING STUDY

S. CANNISTRARO and P. L. INDOVINA

Gruppo di Biofisica Molecolare, Dipartimento di Fisica dell'Università,
Perugia, Italy

and

Laboratorio di Fisica, Istituto Superiore di Sanità, Roma, Italy

Abstract:

Ceruloplasmin, a paramagnetic copper containing protein, has been spin labeled with different nitroxide spin labels in order to study its molecular dynamics and to gain further information about its interaction with other biosystems. Spin labeling with a maleimide derivative resulted in an Electron Spin Resonance spectrum which was a superposition of two different absorptions due to paramagnetic species in different microenvironments. The first one, a three line isotropic spectrum, is due to a fast moving spin label (with a rotational correlation time $\tau_c \approx 10^{-9}$ s); the second one is an anisotropic, asymmetrical signal arising from an immobilized spin in a slow motion domain ($\tau_c = 10^{-7}$ s). The assumption of a spherical shape for the molecule provided, through the Stokes-Einstein relation, an estimate of the molecular radius value consistent with small angle neutron scattering measurements. The interaction with other biosystems, as deduced from the protein molecule dynamics, is discussed.

PACS NUMBERS: 76.30 -v; 87.15 -v.

Introduction

Ceruloplasmin (CP) is a copper containing protein which shows many interesting spectroscopic and biophysical aspects⁽¹⁻³⁾ and probably a superconducting behaviour at high temperature⁽⁴⁾. A CP molecule weighs about 132.000 daltons and bears about seven intrinsic Cu^{2+} ions. A careful reinvestigation by computer simulation⁽⁵⁾ has shown that 44% of the total copper content is in a paramagnetic state, the overall Electron Spin Resonance (ESR) spectrum at low temperature (77K) being interpreted in terms of a superposition of three different spectra arising by the so-called Type I_a, Type I_b and Type II Cu^{2+} ions. Owing to the different crystal field symmetries and/or strengths provided by the protein ligands, the Cu^{2+} types show distinct spectroscopic features (optical absorption intensities, g- and hyperfine tensors and so on). The rest of the copper ions are in a diamagnetic state (ESR-silent) and probably consist of Cu^{2+} ion pairs with extensive antiferromagnetic coupling⁽¹⁾. At the very beginning of the present work we thought that the introduction of another paramagnetic species, such as a nitroxide radical of spin $S = \frac{1}{2}$ at a suitable site in the molecule, could have resulted in a dipolar perturbation of this antiferromagnetic coupling thus providing information about these Cu^{2+} ESR silent ion pairs. Even though such a perturbation is not observed, at least with the nitroxide spin labels used throughout this work, the spin labeling approach allowed us to obtain interesting structural - dynamic information on CP, which can also be connected with its interaction with some biological substrates.

Among other results, calculation of the macromolecule rotational correlation time allowed us to estimate, through the Stokes-Einstein relationship, a value of $39.5 \pm 2 \text{ \AA}$ for its radius. This value was found to be consistent with that obtained by small angle neutron scattering measurements⁽³⁾.

Experimental methods

Human CP was purchased from Sigma (Lot: 33F-93902), as a 5% solution in 0.25M NaCl and 0.05M sodium acetate, its concentration being determined spectrometrically to be $2.06 \cdot 10^{-4}$ M. Nitroxide spin labels were purchased from Syva, Palo Alto. Covalent binding of spin labels to CP was achieved by incubation (10 hours at 5 °C) of 1 ml of protein solution with 1 ml of nitroxide dissolved at 50-fold molar excess in the same buffer as CP. Unbound spin label molecules were removed by exhaustive dialysis against buffer. All the experiments were performed at pH=7. To run ESR spectra at controlled room temperature the aqueous samples were introduced into capillary tubes (1 mm i.d.). This choice obeyed the conflicting requirements of highest filling factor and lowest dielectric loss due to aqueous samples (the TE₁₀₂ rectangular resonant cavity used shows a minimum in the electric field in the center of its filling hole). The capillary sample was then placed in a standard ESR tube, which was in turn placed in the ESR variable temperature dewar insert filling the central hole of the resonant cavity. ESR experiments at low temperature were conducted as previously described⁽⁵⁾.

ESR spectra were recorded by an X-band Varian E-109 spectrometer equipped with a variable temperature accessory. A 100 kHz modulation frequency was used for phase-sensitive detection. Instrumental settings which gave optimum sensitivity with least distortion of line shape were 1.25 Gauss (G) modulation amplitude, 10 mW incident microwave power, 100 G scanning in 8 min and 0.250 s time constant. Quantitative determinations of paramagnetic species were performed by double integration of the dX''/dH curve displayed by the ESR recorder and by comparison with calibrated paramagnetic standards. ESR data acquisition was performed on an HP 86A microcomputer, through an home-made interface connected to an IEE 488 bus. To calculate the experimentally observed g-factors and the hyperfine splittings, a magnetic field calibration was performed with the Magnion Precision NMR Gaussmeter. Model G-502, the microwave frequency was then determined by the relation-

ship: $\nu = g_{\text{DPPH}} \beta H/h$, where $g_{\text{DPPH}} = 2.0036$. Sample viscosity measurements were performed with an Ostwald-type viscosimeter. Optical absorption measurements were made by a Mod. 360 Shimadzu spectrophotometer.

Results and discussion

The ESR spectra at 20 °C of the maleimide spin label (3MAL) in a diluted aqueous solution and of the same spin label but covalent bound to CP are shown in Fig.1, patterns a and b respectively. The chemical formula of the nitroxide radical is also shown. The spectra are displayed as the first derivative of the resonant paramagnetic susceptibility dX''/dH .

In general the spin Hamiltonian of a nitroxide radical of spin $S=1/2$ is given by:

$$\mathcal{H} = \beta \vec{H} \cdot \hat{g} \cdot \vec{S} + \vec{I} \cdot \hat{A} \cdot \vec{S} \quad (1)$$

The first term describes the Zeeman interaction of the spin with the externally applied magnetic field H and the second term gives the hyperfine interaction of the unpaired electron with the ^{14}N nucleus ($I=1$). The success and importance of the spin labeling method of studying the structure and dynamics of macromolecules is based on the fact that the \hat{g} and \hat{A} tensors are anisotropic, making the ESR spectra critically dependent on the orientation of the spin label.

When the spin labels are allowed to tumble rapidly in an isotropic way, the spin Hamiltonian (1) becomes time-dependent and one can write⁽⁶⁾:

$$\mathcal{H}(t) = \mathcal{H}_0 + \mathcal{H}_1(t) \quad (2)$$

where

$$\mathcal{H}_0 = \beta g_{\text{iso}} \vec{H} \cdot \vec{S} + A_{\text{iso}} \vec{I} \cdot \vec{S} \quad (3)$$

and

$$\mathcal{H}_1 = \beta \vec{H} \cdot (\hat{g} - g_{\text{iso}}) \cdot \vec{S} + \vec{I} \cdot (\hat{A} - A_{\text{iso}}) \cdot \vec{S} \quad (4)$$

The isotropic values, g_{iso} and A_{iso} , of the tensor \hat{g} and \hat{A} , are given by:

$$g_{iso} = \frac{1}{3} (g_{xx} + g_{yy} + g_{zz}) \quad (5)$$

$$A_{iso} = \frac{1}{3} (A_{xx} + A_{yy} + A_{zz}) \quad (6)$$

If the molecular motion is fast enough, so that $|\mathcal{H}_1(t)|\tau_c \leq 1$, $\mathcal{H}_1(t)$ can be treated as a time-dependent perturbation (6) and gives rise to line broadening through the induction of transitions between electronic and nuclear spin states and modulation of energy levels.

The line positions can be calculated from Eqn. (3) which yields a three line spectrum whose splitting is A_{iso} and which is centered at g_{iso} (7,8). If the motion is very fast ($\tau_c < 10^{-11}$ s), the spectrum will consist of three sharp lines of equal height. This is the case in Fig. 1a where the spectrum of a diluted aqueous solution of 3MAL is shown.

As the motion becomes progressively slower (i.e. by increasing the viscosity of the medium or by branching the spin label to a bigger molecule), there is a differential broadening of the lines while the line positions remain constant (provided that the label still tumbles in the fast motional region: $\tau_c \leq 5 \cdot 10^{-9}$ s). For values of $\tau_c > 5 \cdot 10^{-9}$ s (slow motional region) a distortion of the line positions and lineshape is observed and a break-down of the time-dependent perturbation approach occurs (7).

It is clear that paramagnetic spin labels tumbling in both motional regions contribute to the ESR spectrum of Fig. 1b. Spectra of this type are a composite of two types (9): one, a three line isotropic spectrum, is due to a fast moving or weakly immobilized (labeled W) spin label, while the other is an anisotropic signal arising from strongly immobilized spin labels (labeled S) in a slow motional domain.

Going back to the fast motional situation, since the spin label is tumbling randomly, $\mathcal{H}_1(t)$ is a random function of time and the autocorrelation function of $\mathcal{H}_1(t)$:

$$G(\tau) = \overline{\mathcal{H}_1(t) \mathcal{H}_1(t+\tau)} \quad (7)$$

measures the persistence of the fluctuations in the system. This correlation function depends on the particular model adopted for molecular reorientation. Brownian diffusion is generally a good description for the motional behaviour of macromolecules such as proteins in a solution (7,10). In this case an exponential decay of the autocorrelation function (7) is observed:

$$G(\tau) = \overline{|\mathcal{H}_1(t)|^2} e^{-\tau/\tau_c} \quad (8)$$

If the spin label is approximated to by a rigid sphere of radius R rotating in a medium of viscosity η , then a rotational Stokes Einstein relationship (6,10) yields:

$$\tau_c = \frac{4\pi}{3} \frac{\eta R^3}{kT} \quad (9)$$

The relaxation processes induced by the random function $\mathcal{H}_1(t)$ are determined by the spectral density $J(\omega)$ which is the Fourier transform of $G(\tau)$ and according to Eqn. 8 takes the form:

$$J(\omega) = \int_{-\infty}^{\infty} G(\tau) e^{i\omega\tau} d\tau = \frac{2\tau_c}{1+\omega^2\tau_c^2} \overline{|\mathcal{H}_1(t)|^2} \quad (10)$$

Redfield (11) has given an exact derivation of the spin-spin relaxation time, T_2 , which governs the line width of the ESR absorptions in terms of $J(\omega)$ obtaining the expression:

$$T_2(M_I) = a + bM_I + cM_I^2 \quad (11)$$

where M_I denotes the nitrogen nuclear spin quantum numbers.

For practical reasons it is more convenient to work in terms of linewidths in magnetic field units; Eqn. 11 can then be rewritten:

$$\Delta H(M_I) = A + BM_I + CM_I^2 \quad (12)$$

where ΔH is the peak-to-peak linewidth. For a Lorentzian line shape the peak-to-peak height h varies with the inverse square of ΔH so that:

$$B = \frac{1}{2} \Delta H(\omega) \left[\sqrt{\frac{h(\omega)}{h(\omega)}} - \sqrt{\frac{h(\omega)}{h(-\omega)}} \right] \quad (13)$$

$$C = \frac{1}{2} \Delta H_{(0)} \left[\sqrt{\frac{h(0)}{h(-1)}} + \sqrt{\frac{h(0)}{h(-1)}} - 2 \right] \quad (14)$$

Finally, taking into account the explicit expression given for the B and C terms (12) the following useful relations can be obtained:

$$\tau_c = 1.22 \cdot 10^{-9} \text{ s} \quad (15)$$

$$\tau_c = 1.19 \cdot 10^{-9} \text{ s} \quad (16)$$

Eqns. 13-16 allow two independent determinations of the rotational correlation time for isotropic fast motion from the experimental spectra. Then, from the isotropic component (W) of the 3MAL-CP spectrum we measured a τ_c of $1.96 \cdot 10^{-9}$ s by using Eqn. 15 while Eqn. 16 gave $\tau_c = 2.10 \cdot 10^{-9}$ s. These values indicate that the spin labels are bound to the CP molecules at sites which allow the labels to retain a large degree of rotational freedom with respect to the tertiary structure of the protein. It should be noted that 3MAL nitroxides show a specific chemical reactivity towards the free SH groups of the protein. Moreover, since the g and A values measured from the isotropic component of the 3MAL-CP spectrum are consistent with a spin label situated in a polar medium (7,10), it can be inferred that these SH groups are located at the surface of the molecule and are freely exposed to the solvent. The difference between the two correlation times calculated from Eqns. 15 and 16 may arise from a slight anisotropy in the motion of the bound labels (7). It turns out that these kinds of bound spin labels are very sensitive reporters of the microenvironment around their binding sites. In other words, even a slight change in their degree of rotational freedom, as induced for example by a conformational variation of the macromolecule or subsequent to a molecular interaction with another biosystem, would immediately be registered as a change in the ESR line widths and heights and hence in the correlation time. In this connection, we have performed some experiments that will be reported later.

The calculation of the correlation time of the bound spin labels which give rise to the asymmetrical anisotropic signal (powder-like spectrum)

labeled S in Fig. 1b, is not as simple as the previous one. Since $H_1(t)$ does not fluctuate rapidly enough, the perturbation theory of Redfield is no longer valid. In this case no direct theoretical expression can be found for τ_c and it is necessary to simulate the spectra, both position and line width depending on τ_c . Two approaches have been developed to calculate the line shape of the ESR spectra (10,13). The simpler one (13) takes into account the solution of the Bloch equations, describing the time derivative of the macroscopic magnetization M, coupled to a diffusion term. Assuming an isotropic Brownian diffusion model, a numerical solution of the Eqn:

$$\frac{d\vec{M}}{dt} = \gamma \vec{M} \wedge \vec{H} - \frac{1}{T_1} (\mu_z \vec{I} + \nu \vec{J}) - \frac{1}{T_1} (M_z - M_0) \vec{K} + D \nabla^2 \vec{M} \quad (17)$$

allowed the authors (13) to express quantitatively a dependence of the resonance positions of the outer hyperfine extrema (S_1 and S_3 in our case) on rotational motion. In practice, the correlation time of the strongly immobilized spin labels can be determined by measuring the high field hyperfine component (S_3) position as a function of viscosity η and extrapolating to infinite viscosity. The difference δH between its position for a solution of infinite viscosity and that for the aqueous solution at 20 °C is used to determine the rotational correlation time. The addition of sucrose to the spin labeled CP solution was used to vary the viscosity. Theoretically, $\delta H(\tau_c)$ is proportional to $\tau_c^{-2/3}$; we have therefore, in Fig. 2, plotted δH as a function of $(\frac{T}{\eta})^{2/3}$ for the 3MAL labeled CP. From a least squares fit of data, we have found that the extrapolated shift δH is 1.2 G. According to the plot shown by McCalley et al. (13), this value corresponds to a correlation time of 10^{-7} s. Now, since these bound spin labels have no residual rotational motion with respect to the protein tertiary structure (13) (its spectrum at 20 °C being very similar to that obtained at -195 °C where the matrix is very rigid; see also Fig. 3) this correlation time contains information about the tumbling of the whole biomolecule. Then, under the assumption of a spherical shape for the CP molecule, Eqn. 9 could provide a reliable

estimate of its radius. This relationship is temperature and viscosity dependent, so care was taken to keep the temperature constant (20 °C) throughout all the experiments. The viscosity measurements were done with an Ostwald viscosimeter under exactly the same temperature conditions, sample concentration and composition as in the ESR experiments. By this way, a radius of 39.5 ± 2 Å was obtained for the globular CP molecule. This value agrees quite well with the one previously measured by small angle neutron scattering (3).

It should be noted that repeated standard biochemical tests performed on the spin labeled protein indicated that its enzymatic activity was not impaired. This indicates that neither steric hindrance nor chemical modification is introduced at the protein active site by spin labeling. The low temperature ESR spectrum of the spin labeled CP compared with that of CP alone is shown in Fig.3 (a and b respectively). The ESR spectrum of CP arise from its intrinsic paramagnetic Cu^{2+} ions whose spin Hamiltonian parameters have been widely discussed (1,5). Spin labeled CP shows exactly the same ESR pattern as that arising from the Cu^{2+} ions, but additionally displays the spectral features of bound spin labels which are, of course, all strongly immobilized in the frozen matrix.

Such a low temperature experiment was also done in the attempt to detect a dipolar interaction between the Cu^{2+} ions and the nitroxide spins, as previously mentioned. However we failed to observe such an interaction even in the half field region (not shown) where $\Delta M_S = \pm 2$ forbidden transitions may be seen for a triplet state ($S=1$) (6). In order to determine the number of spin label molecules bound to one CP molecule, we simulated the spectrum of Fig.1b as reported by Jost and Griffith (14) using a calibrated concentration of 3MAL. In this way, we found that 3 molecules of 3MAL are bound to each CP molecule: two of them turn out to be weakly immobilized and the third strongly immobilized. This result is consistent with the

previous report indicating that 3 free sulphhydryl (SH) groups are present in the protein (1).

On the other hand, it has been observed that the low temperature EPR spectrum of Cu^{2+} -CP undergoes slight changes as a function of the solution pH value. In this respect it has been postulated that small conformational changes, induced by pH variations, could modulate the symmetry and/or the strength of the crystal field sensed by the paramagnetic ions (5). To test this hypothesis we investigated the dependence on the pH of the correlation time τ_c of the rapidly tumbling spectral component and the separation, $2A_{zz}$, of the outer components S_1 and S_3 of the strongly immobilized label. The results shown in Fig.4 exhibit a marked increase in the correlation time and in the $2A_{zz}$ value when the pH is brought down to 5. This is just the value at which the low temperature spectroscopic change is observed (5). Results in Fig. 4 could be interpreted in terms of a pH-dependent conformational change which the protein undergoes, this change affecting the mobility of both the weakly immobilized labels and of the biomolecule in its entirety.

Several biosystems have been indicated as interacting with CP in order for an enzymatic or a physiological activity to be performed. A close molecular interaction with Fe^{2+} ions and transferrin molecules has been recently postulated (15). Moreover selective interaction of CP with ferritin, an iron storage protein, has been suggested (16). The spin labeling approach could be used to detect such an interaction if the labeled sites are involved in the bimolecular process. In this case the height ratio S_1/W_1 may also be affected (9), this fact indicating that some weakly immobilized labels become strongly immobilized after the interaction of CP with the substrate, thus contributing to the intensity of the S components. We have performed some ESR experiments to study the effect of all the three above mentioned substrates. In particular we have

taken into account the variation of τ_c , $2A_{zz}$ and of the ratio S_2/W_1 of spin labeled CP on addition of these substrates. We found that only the presence of ferritin led to an effect on the rotational dynamics of CP as registered by a 30% increase in S_2/W_1 ratio. This confirmed the occurrence of a close molecular interaction between the two proteins.

Conclusions

The use of the spin labeling approach to study the molecular dynamics of ceruloplasmin has provided us with a number of interesting pieces of information. The most significant new finding concerns the molecular radius of the globular protein. By assuming a spherical shape for the CP and calculating the rotational correlation time for the strongly immobilized spin labels we found a molecular radius of $39.5 \pm 2 \text{ \AA}$. However some criticism could be made of the calculation method. In the first place, expression (9) is derived for a rigid sphere model for the protein; actually, proteins in solution may undergo an extensive interaction with the solvent and in some cases a hydrated layer should be considered. Consequently, the microviscosity at the protein surface may fluctuate significantly and differ from the bulk viscosity; this fact may affect the value of R obtained through Eqn. 9 quite appreciably. Secondly, the very assumption of a spherical shape, instead of an ellipsoidal one, may be misleading. Nevertheless, the present value of R was found to be in good agreement with that obtained by small angle neutron scattering ($R = 42.6 \pm 3 \text{ \AA}$)⁽³⁾. This may suggest that deviations from the assumed model might induce a variability in the R value ranging within the experimental errors. Another important finding concerns the CP conformational change observed at low pH which is detected as a change in the rotational dynamics of the bound labels. This result can be related to the already observed change in the ESR hyperfine pattern due to the Cu^{2+} ions intrinsically contained by the protein^(1,5).

Finally changes in the spin labeled protein rotational dynamics have provided unambiguous evidence for the occurrence of a molecular interaction with ferritin, an interaction which probably has some quite significant biochemical importance⁽¹⁶⁾.

Acknowledgements

This work has been partly supported by CNR and MPI grants. The collaboration of Dr. F. Ianzini at an early stage of the work is gratefully acknowledged. Thanks are due to M.R. Mencarini for typing the manuscript and to Prof. D. Boothman for careful reading of the manuscript.

References

1. J.A. Fee: Structure & Bonding, **23**, 1 (1975) and references therein.
2. A.S. Brill: "Transition Metals in Biochemistry" (Springer Verlag, N.Y., 1977).
3. S. Cannistraro and F. Sacchetti: Physics Lett., **101A**, 175 (1984).
4. G. Giacomini, C. Di Mauro, S. Onori and S. Cannistraro: "Biological Effects and Dosimetry of Static and ELF Electromagnetic Fields" ed. by M. Grandolfo, S.M. Rindi and S.M. Michaelson (Plenum press, N.Y., 1984).
5. G. Giugliarelli and S. Cannistraro: Il Nuovo Cimento (1984) submitted.
6. A. Carrington and A.D. McLachlan: "Introduction to Magnetic Resonance" (Harper, N.Y., 1969).
7. M.A. Hemminga: Chem. Phys. Lipids, **32**, 323 (1983).
8. C. Emiliani and S. Cannistraro: Il Nuovo Cimento, **2D**, 1203 (1983).
9. H. Schneider and I.C.P. Smith: Biochim. Biophys. Acta, **249**, 73 (1970).
10. J.H. Freed: "Spin Labeling: Theory and Applications", ed. by L.J. Berliner (N.Y., 1976) vol. I p. 53.
11. A.G. Redfield: Adv. Magn. Reson., **1**, 1 (1966).
12. T.J. Stone, T. Buckman, P.L. Nordio and H.M. McConnell: Proc. Natl. Acad. Sci. USA, **54**, 1010 (1965).
13. R.C. McCalley, E.J. Shimshick and H.M. McConnell: Chem. Phys. Lett., **13**, 115 (1972) and references therein.
14. P. Jost and O.H. Griffith: "Spin Labeling: Theory and Applications", ed. by L.J. Berliner (N.Y., 1976) vol. I p. 251.
15. S. Cannistraro, F. Ianzini and P.L. Indovina: Studia Biophysica, **86**, 163 (1981).
16. R.F. Boyer and B.E. Schori: Biochem. Biophys. Res. Comm., **116**, 244 (1983).

(66)

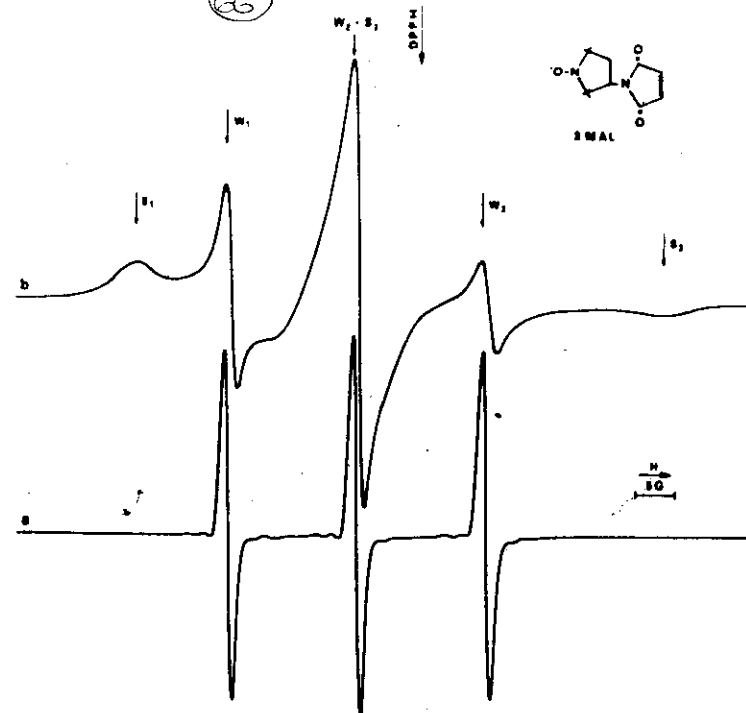
Legend to Figures

Fig.1 Room temperature (20°C) ESR spectrum of: a) 3MAL spin label dissolved in water at $2 \cdot 10^{-4} M$ concentration; b) 3MAL-spin labeled human CP in aqueous solution (10^{-4}).

Fig.2 Plot of ΔH (see text) as a function of $(T/\eta)^{2/3}$ for 10^{-4} spin labeled CP.

Fig.3 Low temperature (77K) ESR spectrum of: a) an aqueous solution ($10^{-4}M$) of human CP; b) an aqueous solution of 3MAL-spin labeled human CP.

Fig.4 Plot of the τ_c related to the weakly immobilized spin labels and of the separation $2A_{zz}$ of the outer components of the strongly immobilized labels vs. the pH value of the CP solution ($10^{-4}M$)



(S. LAM & S. LAM, JR. 1997) FIG. 1

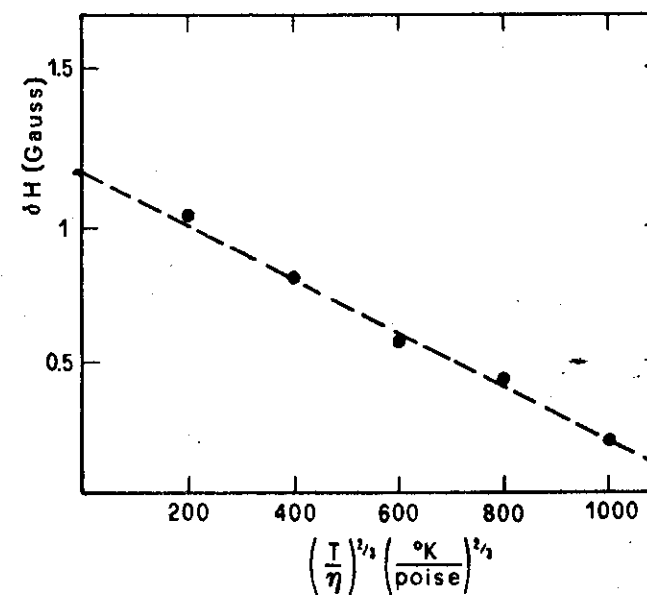
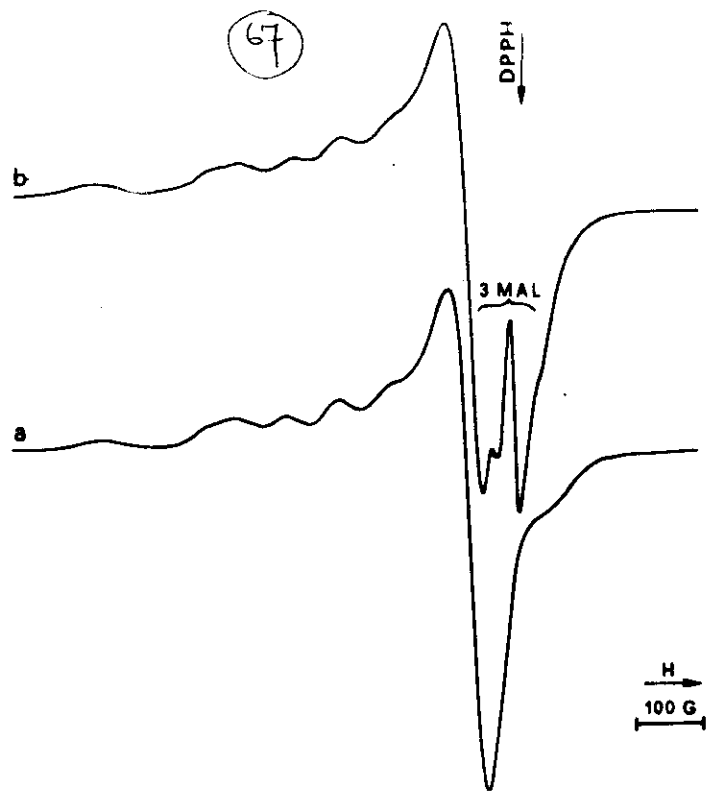
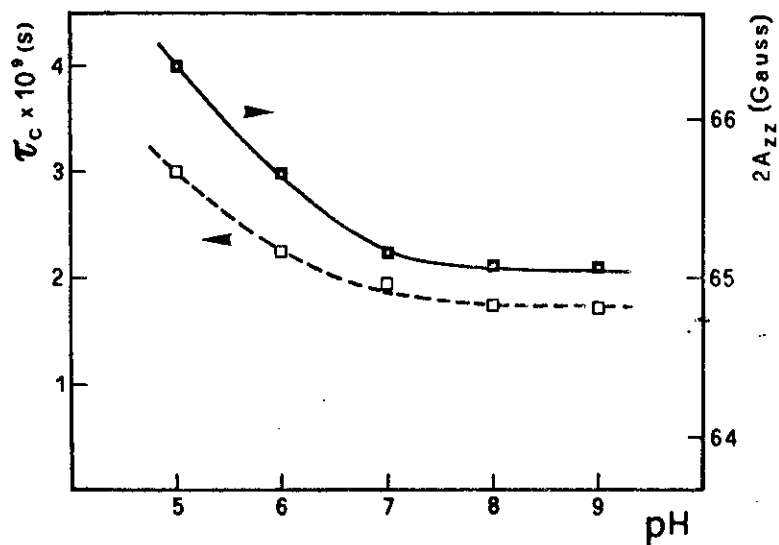


FIG. 2



(S. LAMNISTARIS, P.L. INVERNIZI) FIG. 3



(M. ESTEYRADO, P.L. INVERNIZI) FIG. 4

Riassunto

La ceruloplasmina, una proteina umana contenente ioni Cu^{++} paramagnetici, è stata marcata con differenti spin labels per studiarne la dinamica molecolare e la sua interazione con altri biosistemi. Il marcaggio mediante spin labels di tipo maleimidico ha portato ad uno spettro di Risonanza Elettronica di Spin composto da due differenti gruppi di righe dovuti a specie paramagnetiche in differenti microambienti. Il primo segnale è costituito da un tripletto isotropico dovuto ad uno spin label in rapida rotazione ($\tau_c \approx 10^{-9}\text{s}$), mentre il secondo è alquanto asimmetrico (anisotropico) e deriva da uno spin label ruotante in un dominio temporale piuttosto lento ($\tau_c = 10^{-7}$). L'assunzione di una forma sferica per la proteina in soluzione ha portato, attraverso la relazione di Stokes Einstein, ad una determinazione del raggio molecolare in buon accordo con il risultato di misure di diffrazione a basso angolo di neutroni. Viene inoltre discussa l'interazione con altri biosistemi come desunta dalla dinamica molecolare della proteina.

ELECTRON PARAMAGNETIC RESONANCE STUDY OF STORAGE EFFECTS ON CERULOPLASMIN IN HUMAN SERUM COMPARED WITH PURIFIED CERULOPLASMIN IN AQUEOUS SOLUTION

S. ONORI, A. ROSATI, and S. CANNISTRARO*

Laboratorio delle Radiazioni, Istituto Superiore di Sanità, Viale R. Elena, 299, Rome; and *Gruppo di Biofisica Molecolare, Istituto di Fisica, Università di Perugia, Perugia, Italy

The EPR signal amplitude of human serum ceruloplasmin shows significant changes as a function of time and temperature during storage. The same behavior occurs with aqueous solutions of purified ceruloplasmin. From the observation that the spectral lines of the EPR signal of ceruloplasmin from unmanipulated serum are identical to those coming from purified ceruloplasmin, we conclude that only type I Cu²⁺ of ceruloplasmin are involved in the signal changes. A temperature-dependent electron shift toward type I Cu²⁺ paramagnetic centers, occurring via the type II and type III Cu²⁺ species of the protein, is believed responsible for the process. The possible origin of the reducing electrons is discussed. A procedure to obtain reproducibility of recording of EPR spectra of ceruloplasmin in physiological fluids is proposed.

INTRODUCTION

Ceruloplasmin (CP), a serum protein containing copper, is reported to increase during pregnancy¹⁻³ and during several pathological states.⁴⁻¹⁰

Its paramagnetism, deriving from the presence of two spectroscopically distinguishable Cu²⁺ species, type I Cu²⁺ and type II Cu²⁺,¹¹ allows the protein to be studied by electron paramagnetic resonance (EPR). Quantitative determinations of the CP level in human serum have been performed almost routinely by this spectroscopic technique.^{3,5,7,9,10} However, in the course of an EPR study on the paramagnetic species present in human sera from various pathological states, we surprisingly found significant fluctuations in the CP signal size from the same sample, dependent upon the storage temperature range, while the other paramagnetic species remained unaltered under the same conditions.

The growing importance currently attributed to quantitative determinations of CP in

pathology on the one hand, and the little information available on the molecular aspects of this protein on the other, led us to investigate in more detail the conditions, the dynamics, and the origins of such signal variation.

Working along those lines, we extended the EPR analysis to aqueous solutions of purified human CP, thus ascertaining that:

(1) The spectroscopic constituents of the CP EPR signal from unmanipulated human serum are identical to those from purified human CP.

(2) A significant fluctuation is registered also in the peak-to-peak signal height of purified human CP when submitted to the same conditions.

(3) Only type I (blue) copper ions are involved in the observed signal variation.

(4) Adding fluoride to the solutions prevents EPR signal fluctuation due to the CP.

It was concluded from the experiments that a temperature-dependent electron shift is probably responsible for the fluctuation of the CP signal.

MATERIALS AND METHODS

Blood was withdrawn from patients by venous puncture and centrifuged immediately to prepare serum samples.

Aqueous solutions of purified human CP were prepared by dissolving commercial human CP (Sigma or Seva) in 0.2 M sodium acetate buffer, pH 5.5. Concentrations of CP were determined by optical absorption using $\epsilon_{410} = 10,900$.¹²

The samples were placed in 4.8 mm i.d. precision glass tubes open at both ends and rapidly frozen in liquid nitrogen. Each sample was then removed from its tube by warming the glass surface just sufficiently to allow the cylindrical content to be pushed out. Finally the samples were stored at different temperatures as described below.

To record the EPR spectrum, a sample was placed in an E-246 Varian dewar filled with liquid nitrogen; the dewar then inserted in the resonant cavity. In this way, the signal-to-noise ratio was considerably improved, as previously reported.¹⁰ All samples

were large enough to fill the EPR-sensitive volume of the resonant cavity. EPR spectra were recorded by an X-band Varian spectrometer, model E-4, equipped with 100 kHz frequency modulation. Quantitative determinations of the paramagnetic species were performed both by measuring the peak-to-peak height of the EPR signal and by double integration of the absorption spectrum. An aqueous solution of Cu²⁺-EDTA (1.6 mM) was used as the standard.

To calculate the experimentally observed g factors, a calibration of the magnetic field was performed with a Magnion Precision NMR gaussmeter, model G-502. A sample of DPPH ($g = 2.0036$) was used to determine the operating microwave frequency.

RESULTS

Serum CP. When the EPR spectrum of normal human serum is recorded at 77°K, two main multiplets are encountered: one at $g = 2.05$, due to ceruloplasmin and the other

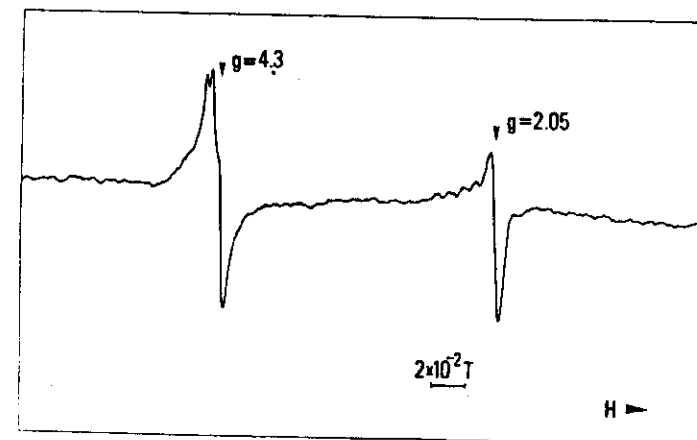


FIGURE 1. EPR spectrum of normal serum recorded at 77°K. Microwave power level: 20 mW. Magnetic field sweep rate: 0.4 tesla in 16 min. Time constant: 3 sec. Modulation amplitude: 5×10^{-2} T.

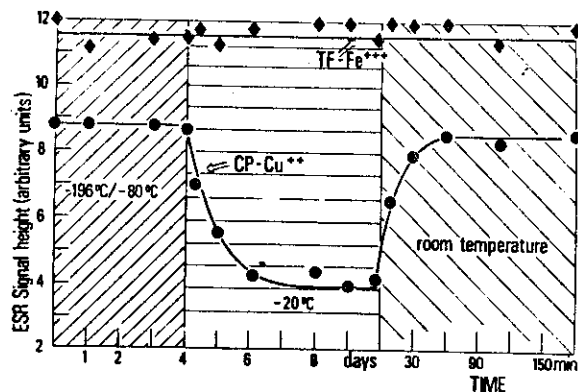


FIGURE 2. EPR signal amplitude of CP and iron transferrin vs. time at different storage temperatures.

at $g = 4.3$ due to iron transferrin^{10,13} (Fig. 1).

Figure 2 shows the behavior of the peak-to-peak amplitudes of these two EPR signals for one particular serum sample when submitted to different storage temperatures. A qualitatively similar behavior was encountered in all the sera investigated, both normal and pathological. In particular, the following may be noted:

(1) Keeping the samples at -196°C or at -80°C for long times (even months) did not result in any change in the signal size.

(2) Storage at -20°C resulted in a progressive decrease of the CP signal height. For all the samples investigated, the minimum value for the signal amplitude, which varied considerably from sample to sample (depending on history of the serum, freezing conditions, etc.), was reached after about 48 h but was never found to be lower than 35% of the initial value.

(3) Successive exposures to air at room temperature restored quickly (within 30 min) the initial amplitude of the CP signal. But if

thawing was performed under an atmosphere of nitrogen, no restoration was observed. Moreover, if the sample had undergone several cycles of freezing and thawing at different temperatures before exposure to air at RT , the original amplitude of the CP signal was not completely restored.

(4) No variation whatever was observed in the iron-transferrin EPR signal.

The same behavior was seen when the experiments were performed with plasma or whole blood. The decrease of the CP signal upon storage of the serum samples at -20°C follows pseudo-first order kinetics, the rate constant of the process being $k = 1.2 \times 10^{-4} \text{ sec}^{-1}$.

To investigate the molecular aspects of the phenomenon more clearly, in particular the nature of the paramagnetic centers involved, we were led to study the behavior of the EPR of purified human CP aqueous solutions under the same conditions.

In order, however, to interpret the results unambiguously, one should be sure that the spectroscopic features of CP in serum are

identical to those of purified CP in solution. In this respect there is a discrepancy among some authors^{14,16} and moreover, the sera studied were manipulated (i.e., concentrated by ultrafiltration). In our case we were able to record, for unmanipulated sera with high CP content coming mainly from pregnant women or tumor bearing patients, a well-

resolved CP EPR spectrum allowing reliable comparison with the spectrum of purified CP in solution.

The two spectra, with their theoretical hyperfine pattern in $g_{\parallel} = 4.3$ region, are shown in Fig. 3. Type II copper, whose presence in serum CP has been controversial,^{14,16} can be easily identified in Fig. 3a by its low-field

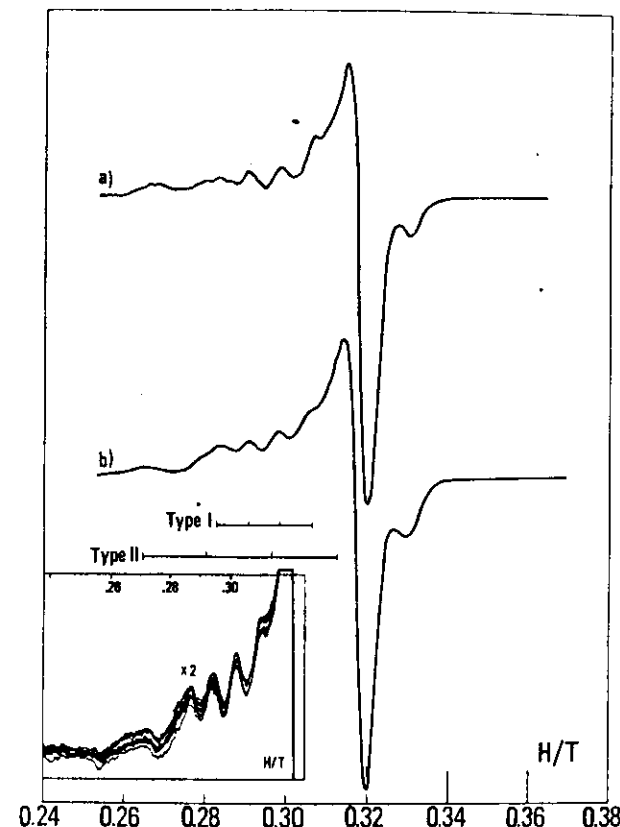


FIGURE 3. EPR spectrum at 77°K in the $g = 2.05$ region of (a) unmanipulated serum from pregnant woman, and (b) aqueous solution of purified human CP (10^{-4} M). Insert: repeated scanning of spectrum a. Microwave power level: 20 mW. Magnetic sweep rate: 0.2 T in 8 min. Time constant: 3 sec. Modulation amplitude: $5 \times 10^{-4} \text{ T}$.

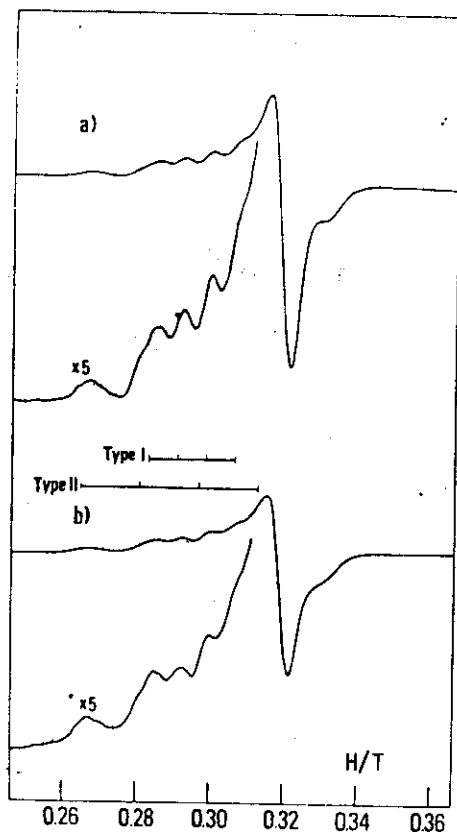


FIGURE 4. EPR spectrum, at 77°K, in the $g = 2.05$ region of (a) aqueous solution purified human CP (10^{-4} M) measured immediately after freezing at 77°K and (b) the sample after having been kept at -20°C for 15 min. Recording conditions as in Fig. 3.

hyperfine line situated at about 0.268 tesla. A repeated scanning of this spectrum is shown in the insert of the same figure. Since type II copper was definitively confirmed to be present in serum CP, we also performed a comparison between the relative amount of paramagnetic centers of this type present in serum CP and the relative amount present in purified CP.

Using the method developed by Vann-gard¹² based on measurement of the area underlying the low-field hyperfine line of $\text{Cu}^{2+}(\text{II})$, we found that in purified CP the amount of $\text{Cu}^{2+}(\text{II})$ corresponds to about 35% of total EPR-detectable copper (i.e., type I plus type II), whereas in our serum samples the amount of $\text{Cu}^{2+}(\text{II})$ corresponds to about 52% of total paramagnetic copper.

Purified CP. Experiments we performed with purified commercial CP in buffer solutions have shown again that the CP signal amplitude undergoes a significant decrease if the samples are stored at -20°C before recording the EPR spectrum.

The situation is seen in Fig. 4. A careful examination of the hyperfine pattern in the $g = 2.05$ region of the spectrum shows that only type I (blue) copper lines (those with the smaller hyperfine splitting, $A_{\text{H}} = 0.05$) are reduced upon storage at -20°C . In particular we ascertained that the process occurs for storage temperature values ranging from -15°C to -65°C .

In this case, the diminution of the signal amplitude lay between 15% and 40% of the initial value, depending on the sample history (type of commercial CP used, freezing procedure, etc.). However, the process occurred much more rapidly than for serum CP. The decrease of the signal of purified CP, at different concentrations, followed pseudo-first order kinetics with a rate constant $k = 8 \times 10^{-3} \text{ sec}^{-1}$. Also in this case, restoration of the initial amplitude of the signal was achieved by exposure of the sample to air at RT.

DISCUSSION

An artificial fluctuation of the EPR signal in the serum, plasma or whole blood samples may, of course, considerably reduce the reliability of EPR data in the study of pathological states.

Horn et al.¹³ have reported that the EPR signal of blood CP increases dramatically during the first 90 min following withdrawal from donors, after which a plateau is reached. This observation led the authors to draw attention to the correct procedure to follow when blood samples are to be analyzed by EPR.

Our data demonstrate quite clearly that a CP EPR signal fluctuation is induced by the storage conditions to which samples of

whole blood, plasma or serum are submitted. The extension of our experiments to purified CP aqueous solutions has allowed us to show, first of all, that the spectroscopic features of CP in serum are identical to those of purified CP. However, the higher content of $\text{Cu}^{2+}(\text{II})$ found in serum CP as compared with that of purified CP may be due to the presence of both the Cu^{2+} -albumin complex and nonspecifically bound $\text{Cu}^{2+}(\text{II})$.¹⁴⁻¹⁷ Probably this copper is the type involved in the transport process performed by CP.¹⁸

Further, our results indicate that fluctuation of the CP EPR signal arises from a reversible temperature-dependent reduction of the type I copper centers of CP. Spectroscopic evidence of this fact is provided by the spectra of Fig. 4, where bleaching of only the type I copper lines is seen upon storage at -20°C . Moreover, this is in agreement with the fact that the maximum diminution of the CP signal amplitude attained in our experiments was about 65% of the initial value. (It should be remembered that type I copper accounts for 67% of total EPR-detectable copper.¹⁹)

Since diminution of the CP signal takes place at sub-zero storage temperatures down to -65°C , the aggregated state seems necessary for the reduction of blue copper, even if this alone is not a sufficient condition for the process to occur.

A diminution of the blue copper optical density at 610 nm was observed by Carrico et al.²⁰ when the temperature of partially reduced CP was decreased below -3°C . To explain this phenomenon, the authors suggested a temperature-dependent electron shift toward blue copper involving the other two types of copper (type II and type III) present in CP. Effectively, they provided evidence that fluoride, which strongly affects type III spectroscopic characteristics, prevents bleaching of the blue (type I) copper absorbance. In analogy, in our EPR experiments we found that adding NaF to the solution before freezing completely pre-

vented diminution of CP EPR signal amplitude.

The restoration of the original signal observed after exposure to air is clearly due to the reoxidation of the reduced blue copper by molecular oxygen.

The reduction of blue copper in CP raises, of course, the question of the source of the electrons. The kinetic data rule out intermolecular electron transfer, but there remain at least two candidate electron-donors; namely, water and the carbohydrate moiety of the protein.²¹

However, electron transfer from the carbohydrate moiety would probably have left on it a radical species susceptible to EPR detection.²¹ We failed to detect any such radical (even at very low microwave powers). On the other hand, the oxidation of water by lactase appears thermodynamically feasible.^{19,22} But since blue copper is not

accessible from the aqueous phase,²³ a situation in which water constitutes the source of electrons would require an electron tunneling or an outer sphere mechanism of electron transfer.²⁴ Experiments attempting to ascertain the role of coordinated water in this process are in progress.

Another question to be answered is why the decrease of the CP signal is much slower in serum than in purified CP. The only hypothesis that, at present, might be put forward is that the presence of some ions can delay the process in serum.

For reliability in EPR data from analysis of physiological fluids containing CP-like serum, plasma, or blood, our results lead us to conclude that after every storage at temperature between -15°C and -65°C, the samples must be left exposed to air for at least one hour at RT before recording the EPR spectrum. □

We thank Prof. P. L. Indovina for many helpful discussions.

REFERENCES

1. M. E. Lahey, C. J. Gubler, G. E. Cartwright, and M. M. Wintrobe. Studies on copper metabolism. VII. Blood copper in pregnancy and various pathological states. *J. Clin. Invest.*, **32**, 329 (1953).
2. M. D. Sean, S. O'Reilly, M. Loncin. Ceruloplasmin and 5-hydroxy-indole metabolism in pregnancy. *Ann. J. Obstet. Gynecol.*, **97**, 8 (1967).
3. M. Brai, M. Messina, M. Brai, G. Moscarelli, P. L. Indovina, and S. Onori. ESR of ceruloplasmin and iron transferrin in human serum during pregnancy. *Fisica Med.*, **2**, 33 (1980).
4. N. R. Hughes. Serum transferrin and ceruloplasmin concentrations in patients with carcinoma, melanoma, sarcoma and cancers of haematopoietic tissues. *Aust. J. Exp. Biol. Med. Sci.*, **50**, 97 (1972).
5. C. Mailer, H. M. Swartz, M. Konieczny, S. Ambegaonkar, and V. L. Moore. Identity of the paramagnetic element found in increased concentrations in plasma of cancer patients and its relationship to other pathological processes. *Cancer Res.*, **34**, 637 (1974).
6. N. Shifrine and G. L. Fisher. Ceruloplasmin levels in sera from human patients with various malignant diseases. *Cancer*, **38**, 244 (1976).
7. T. Pocklington and M. A. Foster. Electron spin resonance of ceruloplasmin and iron transferrin in blood of patients with various malignant diseases. *Br. J. Cancer*, **36**, 369 (1977).
8. A. Scanni, L. Licciardello, M. Trovato, M. Tomirotti, and M. Biraghi. Serum copper and ceruloplasmin levels in patients with neoplasias localized in the stomach, large intestine or lung. *Tumori*, **63**, 175 (1977).
9. M. Foster, L. Fell, T. Pocklington, F. Akinsete, A. Dawson, J. M. S. Hutchinson, and J. R. Mallard. Electron spin resonance as a useful technique in the management of Hodgkin's disease. *Clin. Radiol.*, **28**, 15 (1977).
10. M. Bomba, A. Camagna, S. Cannistraro, P. L. Indovina, and P. Samoggia. EPR study of serum ceruloplasmin and iron transferrin in myocardial infarction. *Physiol. Chem. Phys.*, **9**, 175 (1977).
11. J. Deinum and T. Vanngard. The stoichiometry of the paramagnetic copper and the oxidation-reduction potentials of type I copper in human ceruloplasmin. *Biochim. Biophys. Acta*, **310**, 321 (1973).
12. H. F. Deutsch, C. B. Kasper, and D. A. Walsh. Rapid method for preparation of crystalline human ceruloplasmin from Cohn fraction IV-1. *Arch. Biochem. Biophys.*, **99**, 132 (1962).
13. M. A. Foster, T. Pocklington, J. D. B. Miller, and J. R. Mallard. A study of ESR spectra of whole blood from normal and tumor bearing patients. *Br. J. Cancer*, **28**, 340 (1973).
14. T. Vanngard. Some properties of ceruloplasmin copper as studied by ESR spectroscopy. In *Magnetic Resonance in Biological Systems*. Pergamon Press, Oxford, 1967, p. 213.
15. J. Peisach and W. E. Blumberg. Are the copper sites denatured in purified ceruloplasmin? *Fed. Proc.*, **26**, 834 (1967).
16. L. E. Andreasson and T. Vanngard. Evidence of a specific copper (II) in human ceruloplasmin as a binding site for inhibitory anions. *Biochim. Biophys. Acta*, **200**, 247 (1970).
17. R. A. Horn, E. J. Friesen, R. L. Stephens, W. R. Hedrick, and J. D. Zimbrick. ESR studies on properties of ceruloplasmin and transferrin in blood from normal human subjects and cancer patients. *Cancer*, **43**, 2392 (1979).
18. L. Ryden and I. Bjork. Reinvestigation of some physicochemical and chemical properties of human ceruloplasmin (ferroxidase). *Biochemistry*, **15**, 3411 (1976).
19. J. A. Fee. Copper proteins. Systems containing the "blue" copper center. In *Structure and Bonding*. Springer Verlag, Berlin, 1975, p. 1.
20. R. J. Carrico, B. G. Malmstrom, and T. Vanngard. Anaerobic oxidation-reduction titrations of human ceruloplasmin. *Eur. J. Biochem.*, **20**, 518 (1971).
21. Y. Henry and J. Peisach. Photoreduction of copper chromophores in blue oxidases. *J. Biol. Chem.*, **251**, 7751 (1976).
22. R. Malkin and B. G. Malmstrom. The state and function of copper in biological systems. *Adv. Enzymol.*, **33**, 177 (1970).
23. S. J. Koenig and R. D. Brown. Anomalous relaxation of water protons in solutions of copper-containing proteins. *Ann. NY Acad. Sci.*, **222**, 752 (1973).
24. A. S. Brill. Activation electron transfer reactions of the blue proteins. *Biophys. J.*, **22**, 139 (1978).

(Received January 13, 1981)

Spin Exchange in Nitroxide-Charged Membrane Models: an ESR Method for Detecting Photodynamic Effects.

C. EMILIANI and S. CANNISTRARO

Gruppo di Biofisica Molecolare, Dipartimento di Fisica dell'Università - Perugia

(ricevuto il 26 Gennaio 1983)

Summary. — An electron spin resonance (ESR) method for detecting the photodynamic effects induced in membrane models is described. The method is based on the study of the spin exchange line broadening occurring in nitroxide-charged liposomes before and after visible irradiation in the presence of various photosensitizing molecules.

PACS. 87.20. — Membrane biophysics.

1. — Introduction.

The absorption of photons in the visible region of the electromagnetic spectrum by suitable dye molecules present in biological media triggers a series of photophysical, photochemical and photobiological chain events leading to the so-called *photodynamic action*. This action may be eventually visualized as an oxygen-dependent sensitized photo-oxidation of the biological target. In particular, in ordinary conditions of temperature, the photosensitizing molecules are in the ground electronic state (1D_0) and the absorption of a photon brings the dye molecule to the first excited singlet state (1D_1). Then, besides other depletion processes, intersystem crossing to the triplet state (3D_1) can occur. Since the transition $^3D_1 \rightarrow ^1D_0$ is forbidden, the triplet state of the chromophore molecules is relatively long-lived and it is generally accepted that it promotes the subsequent physico-chemical reactions.

Two major classes of reactions can stem from the excited dye triplets (3). Type-I reactions involve a direct interaction of the triplet dye with the sub-

(¹) K. GOLLINICK: *Adv. Photochem.*, **6**, 1 (1968).

strate, resulting in an induction of free radicals which are susceptible of further interaction with molecular oxygen to give the oxidated substrate. Type-II reactions, on the contrary, involve the transfer of the excitation energy from the triplet sensitizer to molecular oxygen with the formation of singlet oxygen (1O_2). This short-lived excited species is highly reactive and, upon diffusion, may come into oxidative reaction with the substrate.

Many practical and immediate applications may stem from the knowledge of the primary steps underlying the photophysical pathway leading to photosensitization. Moreover, since most of the excited species which are involved in such processes bear a net spin (or they may react with suitable trapping molecules giving paramagnetic species), ESR spectroscopy has been widely used to study in detail the overall photoreaction (^{1,2}).

In the present paper, we describe an ESR method of detecting the photodynamic effects occurring at the level of the lipid phase of a biological-membrane model.

Biological-membrane models, liposomes, have been charged, in the inside aqueous phase, with unpaired electron-bearing molecules (nitroxide spin labels) at an elevated concentration (above 50 mM). The exchange interaction arising from the colliding spins in the restricted area brings to broader ESR lines as compared with those arising from dilute solutions of the same nitroxides. Photodynamic attack promoted by the sensitizer molecules dispersed in the bulk aqueous phase leads to oxidative damage of the phospholipid bilayers charged with the concentrated spins. Then leakage of spin labels across the membrane can occur, resulting in a lowering of the inside concentration and hence in a decrease of the exchange interaction. After all, the overall effect of illumination is that the amplitude of the ESR lines displayed by the spin charged liposomes increases remarkably, while the exchange broadening disappears. The present method allows an immediate measure of changes in liposomal-membrane integrity as induced by photosensitizers.

2. — Experimental methods.

2.1. Preparation of the nitroxide-charged liposomes. — The phospholipid bilayers containing the spin labels were prepared from phosphatidylcholine-

(²) S. CANNISTRARO and A. VAN DE VORST: *Biochim. Biophys. Acta*, **476**, 166 (1977).

(³) S. CANNISTRARO and A. VAN DE VORST: *Biochem. Biophys. Res. Commun.*, **74**, 1177 (1977).

(⁴) S. CANNISTRARO, A. VAN DE VORST and G. JORI: *Photochem. Photobiol.*, **23**, 257 (1978).

(⁵) S. CANNISTRARO, G. JORI and A. VAN DE VORST: *Photobiophys. Photobiophys.*, **3**, 353 (1982).

(⁶) C. EMILIANI, M. DELMELLE, S. CANNISTRARO and A. VAN DE VORST: *Med. Biol. Environm.*, **10**, 351 (1982).

79

dipalmitoyl (DPPC, purchased from Sigma Co.) dissolved in CHCl_3 (1 mg/ml). The lipid solution was evaporated to dryness with a rotary evaporator and dried under vacuum overnight. The dried lipids were then added up with Tris buffer (NaCl 0.15 M, pH 7) containing the 4-amino-2,2,6,6-tetramethylpiperidinoxy (Tempamine, Ega-Chemie product) spin label at various concentrations. Immediately after mixing, the solution was sonicated for five minutes by keeping the temperature above the lipid phase transition of DPPC ($T_c = 41^\circ\text{C}$). Fifteen hours later, the charged liposomes, obtained in this way, were separated from the free spin labels present in the aqueous medium by rapid filtration on a short chromatographic column loaded with Sephadex G-25M (Pharmacia product) and equilibrated with buffer. Minor details are described in (7). The final system is constituted by bilayer vesicles, suspended in the aqueous bulk medium and containing in the inner aqueous phase the concentrated spin labels (fig. 1).

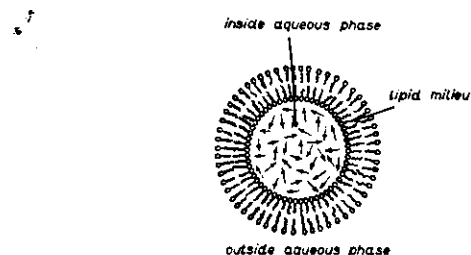


Fig. 1. - Spin label charged liposome.

2.3. Irradiation procedures. - Liposome suspensions were diluted (1:5) and added up with different dyes at a final concentration ranging from 0.01 to 0.1 mM. Solution aliquots were introduced in 100 μl calibrated capillaries ($\varnothing = 1\text{ mm}$), placed in an ESR quartz tube ($\varnothing = 4\text{ mm}$) and then inserted in the Varian E-231 quartz dewar. The dewar tail was placed in the TE₁₀₂ resonant cavity of the ESR spectrometer and irradiation of the samples was performed directly into the cavity, through the built-in grid, by a high-pressure xenon discharge lamp (Osrarn, 150 W), properly focused. The light passed through a cut-off ($\lambda > 350\text{ nm}$) and a water filter to eliminate ultraviolet and infra-red radiations. Under these conditions and a fixed geometry the irradiation light fluence, at the level of the samples, was 6.8 mW/cm², as measured by an EG&G Instr. Photometer.

(7) L. SPORTELLI, G. MARTINO and S. CANNISTRARO: *Bioelectrochem. Bioenerg.*, **9**, 197 (1982).

80

2.3. Electron spin resonance spectroscopy. - ESR measurements were made at $(20 \pm 0.2)^\circ\text{C}$, by an X-band Varian E-109 spectrometer equipped with a variable temperature accessory. A 100 kHz modulation frequency was used for phase-sensitive detection and the peak-to-peak modulation amplitude never exceeded the value of 1 G, to avoid apparent broadening due to overmodulation. The microwave power level was chosen in order to avoid saturation of the absorption, i.e. the ESR line width is mainly determined by the transverse relaxation time (T_2). Calibration of the magnetic field was performed with a Magnion Precision NMR gaussmeter, by using the proton magnetic resonance of water as a standard; the microwave frequency was then determined by the relationship $\nu = g_{\text{DPPH}} \beta_e H/h$, where $g_{\text{DPPH}} = 2.0036$.

3. - Results and discussion.

The nitrogen $2p\pi$ -orbital carries the unpaired electron of the nitroxide molecule NO bond. Then an anisotropic hyperfine interaction with the nitrogen nuclear spin ($I = 1$) should be expected. However, if the spin label molecules are dissolved in a low-viscosity solvent, then the very fast molecular reorientation due to thermal motions averages out the anisotropic term of the spin Hamiltonian (8). The energy levels of the system can be obtained in terms of the isotropic Hamiltonian

$$(1) \quad \mathcal{H}_s = g\beta_e \mathbf{H} \cdot \mathbf{S} + a\mathbf{S} \cdot \mathbf{I}.$$

By treating the hyperfine term as a perturbation on the eigenstates of the Zeeman term, by taking into account the ESR selection rules, the electron and nitrogen nuclear spin quantum numbers, three ESR lines of equal intensity and centred at the fields

$$(2) \quad H_{\pm} = \frac{h\nu}{g\beta_e} \mp \frac{am_i}{g\beta_e}.$$

are to be expected.

Actually, the ESR spectrum related to a diluted aqueous solution (0.005 mM) of Tempamine nitroxide shows three lines of equal heights and equally spaced (fig. 2a)). The isotropic g -value, the isotropic hyperfine splitting constant, a , and the line width, H_{ss} , have been determined to be 2.0069 G, 16.75 G and 1.75 G, respectively.

Figure 2b) shows the ESR spectrum of Tempamine-charged liposomes suspended in the buffer and containing in the inside aqueous phase a nitroxide

(8) P. L. NORDIO: *Spin Labeling: Theory and Applications*, edited by L. J. BERLINER (New York, N. Y., 1976), p. 5.

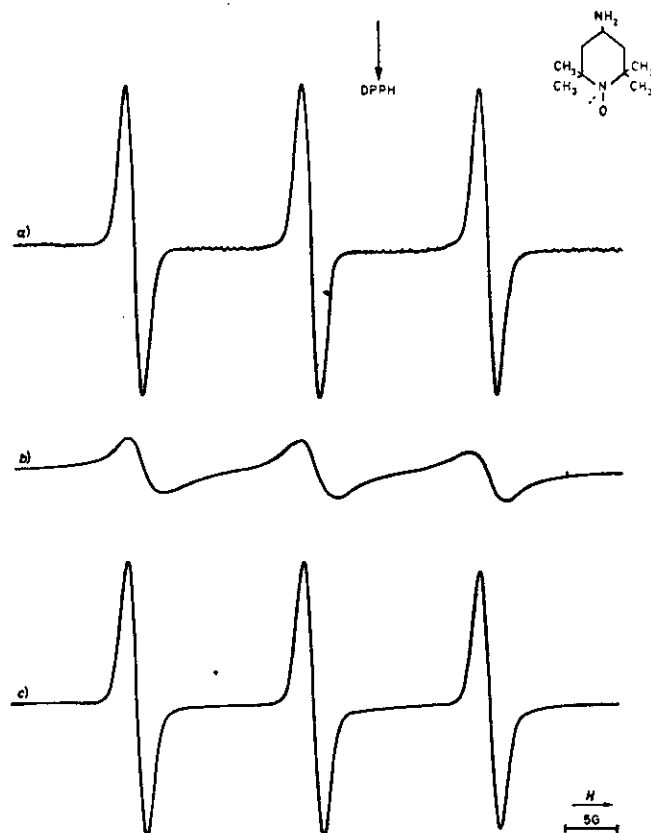


Fig. 2. — Spin exchange effects on the ESR line width in nitroxide-charged liposomes: a) ESR spectrum of aqueous solutions of Tempamine alone (0.005 mM), recorded at 20°C. The chemical structure of the spin label is shown in the upper right-hand side of the figure. Microwave power level 2 mW. Magnetic-field sweep rate 100 G in 8 min. Time constant 0.5 s. Modulation amplitude 1 G. b) ESR spectrum of Tempamine-charged DPPC liposomes suspended in Tris buffer (spin label concentration 0.1 M; pH 7). ESR sets as in a). c) ESR spectrum of Tempamine released from liposomes (same as in b)) by freeze-rupturing. The spectrum has been recorded at a gain 100 times higher than that in a), while all the other conditions remained identical.

concentration of 0.1 M. As can be seen, the three ESR lines are significantly and equally broadened, the peak-to-peak width measuring about 6 G.

Since it has been ascertained, by testing deaerated solutions, that the broadening is not due to a dipolar interaction with paramagnetic molecular oxygen, there remain two possible sources of such a line broadening. As the concentration of the free radicals rises, their unpaired electrons get sufficiently close to one another so they become susceptible to interact via one or both of the two mechanisms. The dipolar interaction between two unpaired electrons (each bearing a spin $s = \frac{1}{2}$), after averaging over the electron co-ordinates, is currently expressed ⁽⁹⁾ by

$$(3) \quad \mathcal{H}_d = S \cdot \hat{D} \cdot S, \quad \text{where } S = S_1 + S_2,$$

The interaction between dipole moments is relatively long range and is determined by their relative orientations and mutual separation. If the two spins reorient, in a magnetic field, at a rate comparable to the frequency corresponding to the energy difference between the electron-electron energy states, line broadening will be observed. If both reorient rapidly in the applied magnetic field, this interaction is averaged to zero regardless of concentration ⁽¹⁰⁾. This occurs in the present case, since in aqueous solutions the correlation time, τ_c , of the nitroxide molecules is lower than $1.2 \cdot 10^{-9}$ s ⁽¹¹⁾.

On the other hand, increasing the nitroxide concentration leads to more frequent radical-radical collision getting consequently more chance that the electronic wave function overlap. An isotropic coupling between the spins S_1 and S_2 , originating from electrostatic interactions which tend to couple the spins into a singlet and a triplet state, must be introduced ⁽¹²⁾. Following the Heitler-London description of the bonding, this interaction is termed exchange interaction and has the form

$$(4) \quad \mathcal{H}_e = JS_1 \cdot S_2 = \frac{1}{2}J(S^2 - \frac{3}{2}), \quad \text{where } S^2 = (S_1 + S_2)^2.$$

Phenomenologically, this electrostatic coupling energy may interchange the spins of the two radicals so that $\alpha\beta$ becomes $\beta\alpha$. The overall effect can be generally discussed in terms of a variation of the transverse relaxation time T_2 , as due to an additional random magnetic field sensed by the spin system under

⁽⁹⁾ A. CARRINGTON and A. D. MCLACHLAN: *Introduction to Magnetic Resonance* (New York, N. Y., 1969), p. 30.

⁽¹⁰⁾ I. C. P. SMITH and K. W. BUTLER: *Spin Labeling: Theory and Applications*, edited by L. J. BERLINER (New York, N. Y., 1976), p. 423.

⁽¹¹⁾ J. H. FREED: *Spin Labeling: Theory and Applications*, edited by L. J. BERLINER (New York, N. Y., 1976), p. 53.

⁽¹²⁾ J. E. WERTZ and J. R. BOLTON: *Electron Spin Resonance, Elementary Theory and Practical Applications* (New York, N. Y., 1972), p. 201.

H_s ⁽¹²⁾. More directly, line broadening has been correlated to the spin exchange frequency, ν_{exch} , by the following relationship ⁽¹⁴⁻¹⁶⁾:

$$(5) \quad \Delta H_{\text{exch}} = \frac{2\hbar}{g\beta_s} \nu_{\text{exch}},$$

where ν_{exch} has been reasonably assumed to be equal to the collision frequency, which depends on the spin label diffusion coefficient, D_{diff} , and on the concentration of the spin labels, C , in agreement with the expression

$$(6) \quad \nu_{\text{exch}} = kD_{\text{diff}}C.$$

The analytical treatment of the phenomenon is somewhat involved and is beyond the aim of the present work. The discussion here presented was just taking aim at supporting the attribution of the line broadening shown in fig. 2b) to a concentration-dependent spin exchange interaction. Actually a linear relationship was obtained by plotting the ESR line width vs. the nitroxide concentration (in the range 50–500 mM) inside the liposomes (plot not shown).

This concentration-dependent line broadening can be used to measure the rate of spin label diffusion across the lipid milieu. At first, the spectrum of fig. 2c) shows a manifold increase of the ESR signal intensity and a concomitant line narrowing, when nitroxides are abruptly released upon liquid-N₂ freeze-rupturing of liposomes. These drastic changes occurring to the ESR spectrum clearly indicate that the membrane models were charged at a high concentration of exchanging spins.

As already mentioned, several dyes are able to promote photodynamic damage on biological targets. The most important targets are, of course, DNA, proteins and cell membranes. In particular, photodynamic effects occurring at the level of the membrane are of utmost importance for the survival of the living system, since the membrane permeability can be severely affected with subsequent lysis of the cell. Besides other detrimental effects, peroxidation of the lipid constituents of the membrane has been shown to be induced by photodynamic sensitizers ⁽¹⁷⁾. Moreover, it has been postulated that this lipid impairment is responsible for the creation of pores in the lipid bilayer and for the consequent osmotic breakdown. In this respect, the spin label charged liposomes would constitute a very suitable model system to follow a possible

⁽¹²⁾ A. G. REDFIELD: *Adv. Magn. Reson.*, **1**, 1 (1966).

⁽¹⁴⁾ C. S. JOHNSON: *Mol. Phys.*, **12**, 25 (1967).

⁽¹⁵⁾ W. PLACHY and D. KIVELSON: *J. Chem. Phys.*, **47**, 3312 (1967).

⁽¹⁶⁾ E. SACKMANN and H. TRAUBLE: *J. Am. Chem. Soc.*, **94**, 4482 (1972).

⁽¹⁷⁾ S. M. ANDERSON and N. I. KRINSKY: *Photochem. Photobiol.*, **18**, 403 (1973).

photodynamic induction of such pores. That is, if such pores are formed, leakage of inside spin labels should occur; consequently a lowering of their concentration in the inside aqueous phase would result in a decreased spin exchange line broadening and, as a result, an increase of the ESR signal will be detected. Actually, this result was obtained by using three different photodynamic agents, i.e. psoralen, hematoporphyrin and chloropromazine (all of commercial origin). The dyes investigated are not able to penetrate into the lipid phase, within at least the range of temperature at which experiments were carried ⁽¹⁸⁾. Moreover, they are photodynamically very active (two of them are currently used in the phototherapy of human diseases) and follow different photoreaction pathways, which have been studied in detail ⁽¹⁹⁾. In particular, hematoporphyrin and psoralen act by both mechanisms (type I and II), while chloropromazine follows only the type-I mechanism.

When one of these dyes was mixed with the charged liposomes and the ESR signal amplitude was plotted as a function of the irradiation time, the results shown in fig. 3 (upper curve) were obtained. After exposure to visible

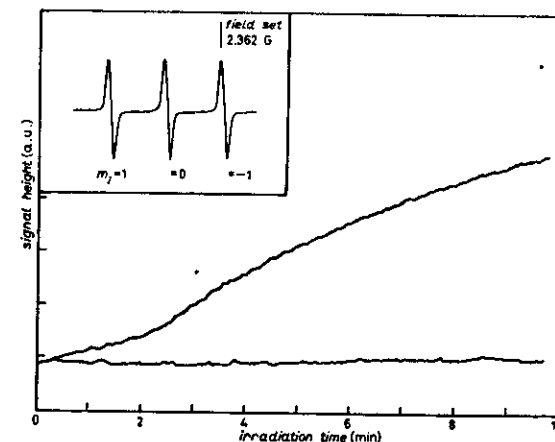
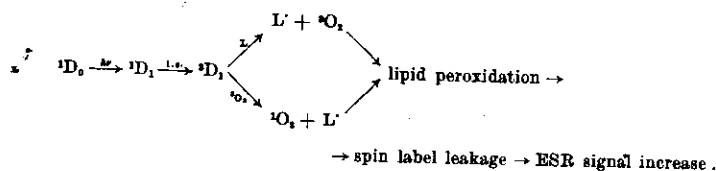


Fig. 3. — Dye-plus-light-sensitized leakage of spin labels from liposomes. ESR signal amplitude was plotted as a function of the irradiation time (the light fluence at the sample was 6.8 mW/cm²). The magnetic field was preadjusted to the maximum of the high-field nitroxide line (see the inset in the same figure) and the ESR signal arising at this field setting was directly recorded vs. the irradiation time. No dark release was observed after mixing of the dyes used with the charged liposomes. Spectrometer gain was held constant during experiment. Other conditions were as in fig. 2, except that the magnetic field was not swept.

light was initiated, spin label release continued at the same rate for about two minutes and then slightly increased.

Qualitatively, the variation of the ESR signal, upon irradiation, was similar for all the dyes studied, even if the rate of release was slightly different (highest for chlorpromazine and lowest for hematoporphyrin).

When the experiments were carried with deoxygenated suspensions of charged liposomes in the presence of dyes, no spin label release was observed (fig. 3, lower curve). This is a clear evidence of the fact that an oxygen-dependent photodamage occurring at the level of the membrane lipid phase is monitored in the experiment represented in the upper curve of fig. 3. Keeping into account the possibility for the dyes used to photoreact by the two different pathways, the results of the experiment could be summarized by the scheme



L[•] indicates the free radicals induced in the lipid moiety, which lead to peroxidation by further reaction with molecular oxygen ([•]O₂) via a type-I mechanism (*).

4. - Conclusions.

The results presented herewith permit to conclude that the photodynamic damage, occurring at the membrane level, can be easily and conveniently detected by monitoring the effect of spin exchange on the ESR lines arising from spin label charged systems.

The method could also be used to follow the effects of ultraviolet light alone, since these more energetic photons are able to induce similar detrimental changes in the lipid bilayer structures. Moreover, the ESR method is susceptible to be applied to naturally occurring membranes, which can be properly resealed after having been charged by the same procedure (erythrocyte ghosts, for example).

Finally, examination of expressions (5) and (6) suggests that further applications of the method could be worked out; for instance, to estimate, within a suitable range, the microviscosity of the inside phase of a cell and/or its volume (a study of this kind is in progress in our laboratory).

This work has been partly supported by the CNR Research Grant No. 82.00176 and by a MPI Research Grant. Thanks are due to Mr. E. BABUCCI for the excellent technical assistance during the design of the irradiation apparatus.

● RIASSUNTO

Si descrive un metodo per la rivelazione degli effetti fotodinamici indotti in modelli di membrane, utilizzando la spettroscopia di risonanza elettronica di spin (ESR). Il metodo è basato sullo studio dell'allargamento di riga dovuto all'interazione di scambio di spin che si ha in liposomi caricati con molecole di nitrossido, prima e dopo l'irraggiamento con luce visibile in presenza di vari fotosensibilizzanti.

Спиновый обмен в мембранных моделях с молекулами закиси азота: метод электронного спинового резонанса для обнаружения фотодинамических эффектов.

Резюме (*). — Описывается метод электронного спинового резонанса для обнаружения фотодинамических эффектов, индуцированных в мембранных моделях. Метод основан на изучении уширения линии, обусловленного спиновым обменом, в липосомах с молекулами закиси азота перед и после облучения в видимой части спектра в присутствии различных фоточувствительных молекул.

(*) Переведено редакцией.

